

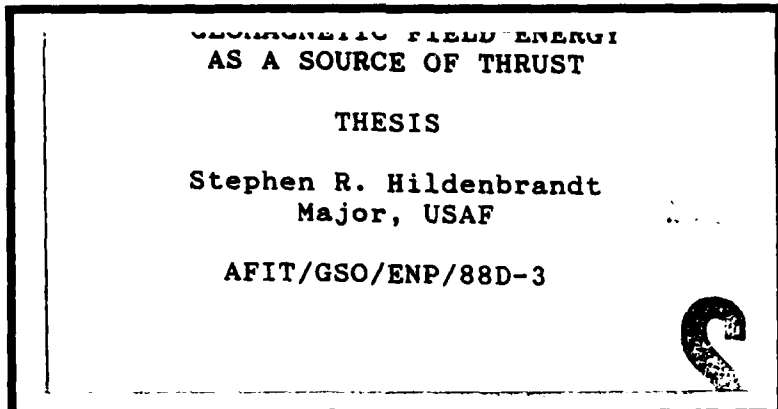
BTM FILE COPY

(1)

AD-A202 567



DTIC
SELECTED
JAN 23 1989
S D
S H



DEPARTMENT OF THE AIR FORCE
AIR UNIVERSITY
AIR FORCE INSTITUTE OF TECHNOLOGY

Wright-Patterson Air Force Base, Ohio

DISTRIBUTION STATEMENT A

Approved for public release
Distribution unlimited

89 1 17 004

(1)

AFIT/GSO/ENP/88D-3

GEOMAGNETIC FIELD ENERGY
AS A SOURCE OF THRUST

THESIS

Stephen R. Hildenbrandt
Major, USAF

AFIT/GSO/ENP/88D-3

DTIC
ELECTED
JAN 23 1980
S & H D

Approved for public release; distribution unlimited

AFIT/GSO/ENP/88D-3

**GEOMAGNETIC FIELD ENERGY
AS A SOURCE OF THRUST**

THESIS

**Presented to the Faculty of the School of Engineering
of the Air Force Institute of Technology
Air University
In Partial Fulfillment of the
Requirements for the Degree of
Master of Science in Space Operations**

Stephen R. Hildenbrandt

Major, USAF

December 1988

Approved for public release; distribution unlimited

Preface

This investigation determines an analytic solution to the force acting on a current loop over a non-uniform expanse of the geomagnetic field. Since the geomagnetic field contains energy and that energy is being used to make attitude adjustments to satellites, it should be possible to use that field energy as a sort of action-at-a-distance space thruster. Although the derivations for the force used a number of simplifying assumptions, the techniques developed are still applicable to a more detailed analytic solution for the force available through the interaction of a current loop and the geomagnetic field.

I am deeply indebted to my thesis advisor, Lt Col Howard Evans, first, for the idea itself, and also, for his continued support and encouragement during the months of contemplation, analysis, evaluation, and writing that this effort represents. Without his superb instructional abilities and insights into the phenomenology of physics, this thesis would not have been completed.

In addition, I would like to recognize my wife Olivia for her understanding and patience throughout my tenure at AFIT and particularly during this thesis effort when the work week seemed to always extend well into the weekend.

Finally, but foremost in deserving recognition, is our Heavenly Father who created the geomagnetic field for a myriad of purposes.



For		I <input checked="" type="checkbox"/>	<input type="checkbox"/>
ion		<input type="checkbox"/>	<input type="checkbox"/>
Distribution/			
Availability Codes			
Dist	Avalil and/or Special		
A-1			

Table of Contents

	<u>Page</u>
Preface	ii
List of Figures	v
List of Tables	vii
List of Symbols	viii
Abstract	xi
I. Introduction	1
Background	1
Statement of Purpose	2
Scope	3
II. Literature Review	4
Scope	4
Orbital Mechanics	5
Magnetostatics	7
Geomagnetic Models	10
Actual Usages of the Geomagnetic Field	13
Conclusion	15
III. Background Theory	16
Introduction	16
Magnetostatics	16
Two-Body Problem	25
Geomagnetic Field Models	30
IV. Development	33
Method Used In Derivation	35
Case I: Loop Parallel to Earth's Surface.	40
Case II: Loop Perpendicular to Earth's Surface	45
Case III: Loop Dipole Parallel to Geomagnetic Field Vector	48
Case IV: An Inertially Oriented Current Loop	52

V.	Application	56
	Perturbations	61
	Magnetic Force Vs Aerodynamic Drag	61
	Solar Radiation Pressure	64
	Magnetic Thruster Operation	66
VI.	Conclusions	68
	Summary	68
	Recommendations	70
	Appendix A: Variation of Parameters	71
	Appendix B: Force Calculation Program	77
	Bibliography	79
	Vita	82

List of Figures

<u>Figure</u>	<u>Page</u>
1. Comparison of a Hohmann Transfer Between Circular Orbit (a) and a Low-Thrust Spiral Transfer Using Infinitesimal Thrust (b)	6
2. Relative Direction of Magnetic Field, Current and Force	8
3. Forces on a Current Loop in a Uniform Magnetic Field	9
4. Forces on the Effective Dipole of a Current Loop in a Uniform (a) and a Non-Uniform (b) Magnetic Field	10
5. Magnetic Field Around a Current Carrying Wire . . .	17
6. Paths of Positive and Negative Electrons Deflected in Opposite Direction in a Magnetic Field	17
7. Paths of Integration in a Magnetic Field	19
8. Schematic Representation of the Biot-Savart Law Where Current Element dL Establishes a Magnetic Field Contribution dB at "P"	20
9. Magnetic Field Along the Axis of a Current Loop . .	21
10. Geometry of Potential Around a Magnetic Dipole . .	22
11. Orbital Elements	29
12. Four Orientations of the Current Loop Relative to the Earth and Each Other	34
13. Case I: Current Loop and Orientation Relative to the Geomagnetic Field and Definitions of dL , ΔR , and $\Delta\theta$	38
14. Case II: Current Loop and Orientation Relative to the Geomagnetic Field and Definitions of dL , ΔR , and $\Delta\theta$	38
15. Case III: Current Loop and Orientation Relative to the Geomagnetic Field and Definitions of dL , ΔR , and $\Delta\theta$	39

16.	Case IV: Current Loop and Orientation Relative to the Geomagnetic Field and Definitions of dL, R, and θ	39
17.	Magnetic Forces for Case I (600 Kilometer Orbit) . .	44
18.	Magnetic Forces for Case II (600 Kilometer Orbit) .	47
19.	Magnetic Forces for Case III (600 Kilometer Orbit) .	51
20.	Magnetic Forces for Case IV (600 Kilometer Orbit) .	55
21.	Operating Regimes of Various Thruster Systems . . .	59
22.	Magnitude of Total Magnetic Force for Case III . .	63
23.	Aerodynamic Drag Vs Solar Radiation Pressure . . .	65
24.	Variation of Parameters Flow Chart	76

List of Tables

<u>Table</u>	<u>Page</u>
I. Comparison of Thrust, Burn Time, and Total Impulse for Various Rocket Engines	60
II. Impulse Over One Orbit for Various Thrusters	60
III. Aerodynamic Drag Force at Various Altitudes	63

List of Symbols

A = Area of the loop
A = Frontal cross-sectional area of satellite (meters²)
a = Equatorial radius
a = Semi-major axis
B = Magnetic field (tesla)
B = Geomagnetic field
 B_ϕ = Magnetic field component in the phi (longitude) direction
 B_r = Magnetic field component in the radial direction
 B_θ = Magnetic field component in the theta (colatitude) direction
 C_d = Drag coefficient
E = Total energy per unit mass
e = Eccentricity
F = Force (newtons)
 F_ϕ = Force in phi (longitude) direction
 F_r = Force in radial direction
 F_θ = Force in theta (colatitude) direction
G = Gravitational constant (newton meters/kilogram²)
 $g^{\circ}n$ = Gaussian coefficient (gauss or nanotesla)
 g^o = First gaussian coefficient (.31 gauss or 30176 nT)
 g_0 = Gravitational attraction (meters/second²)
h = Moment of momentum (angular momentum) vector
I_s = Specific impulse (seconds)
I_t = Total impulse (seconds)
i = Inclination

i = Current (amperes)
k = GM (Gravitational constant)(Mass of the Earth)
k_d = Diffuse coefficient of reflectivity
k_s = Specular coefficient of reflectivity
L = Displacement vector in the current direction (meters)
M = Mass of the earth (kilograms)
m = Mass of the satellite (kilograms)
m = Magnetic pole strength
N = Number of turns of wire in the loop
P_n = Associated Legendre function
p = Solar radiation pressure
q = Charge (coulombs)
R = Vector defining position of a point on the current loop
R = Geocentric distance (meters)
R = Radius of the loop
R = Radial distance from the center of the earth to the center of the current loop
R = Final radius of orbit
R₀ = Vector defining position of center of satellite
R₀ = Initial radius of orbit
R_e = Radius of the earth
 ΔR = Radial difference between the center of the current loop and a point on the current loop
r = Vector from the center of the current loop to a point on the current loop
r = Radial distance from wire
r = Distance of satellite from center of the earth
r = Radius of the current loop (meters)

T = Time of periapsis passage
 τ = Torque
 U = Magnetic potential
 v = Velocity vector of charged particle (meters/second)
 v = Relative velocity of satellite (meters/second)
 w = Argument of periapsis
 x = Distance from the center of the loop to a point along the axis
 y = Separation between magnetic poles
 β = Angle between geomagnetic field vector and current loop dipole
 Γ = Orientation angle
 θ = Angle between vectors μ and B
 θ = Angle between the magnetic field and the magnetic dipole moment of the current loop
 θ = Colatitude/coelevation
 $\Delta\theta$ = Colatitude difference between the center of the current loop and a point on the current loop
 ρ = Atmospheric density
 τ = Longitude of ascending node
 Φ = East longitude from Greenwich
 μ = Magnitude of magnetic moment of loop
 μ = Magnetic dipole moment
 μ_0 = Permeability constant
 Ω = Angle from a reference position on the current loop around the circumference of the current loop

Abstract

This study determines analytic solutions to the interactive net force between the dipole created by a current loop and a non-uniform expanse of the geomagnetic field. A simple dipole approximation is used for the geomagnetic field and it is assumed that the current loop can be maintained in any desired orientation. Analytic solutions are found for four different orientations: the current loop parallel to the earth's surface, the current loop perpendicular to the earth's surface, the current loop dipole parallel to the instantaneous geomagnetic field, and an inertial orientation. A hypothetical satellite-current loop system is discussed and the action-at-a-distance magnetic interaction force is compared to aerodynamic drag and solar radiation pressure. The magnetic force is also compared to the force that some space thrusters produce. In terms of lifetime impulse or total impulse deliverable over one orbit, the magnetic force compares favorably to many thrusters in use today or under consideration.

GEOMAGNETIC FIELD ENERGY AS A SOURCE OF THRUST

I. INTRODUCTION

Background

To accomplish their Department of Defense, scientific, or civil missions, satellites must periodically make attitude adjustments, compensate for orbital perturbations, or maneuver to different orbits. One constraint on their ability to accomplish these tasks, essentially a constraint on their lifetime, is the amount of fuel that can be carried on board. Systems currently in use include conventional chemical rockets, cold gas jets, and, in a few situations, electric propulsion. Once the fuel supply for these activities is exhausted, the satellites cease to be useful and become expensive orbiting junk. An energy source is needed that does not require the carriage of an on-board fuel supply.

The earth is surrounded by a magnetic field; this field contains energy ($B^2/2\mu_0$). By taking advantage of this energy, the amount of on-board fuel consumed by a satellite can be reduced and the lifetime increased. While magnetic torques have been used to adjust satellite attitude (Eller, 1983:315; Kaplan, 1976:196), there has been no attempt to use

the energy contained in the geomagnetic field to change the satellite's orbital elements. Regardless of the means used in moving a satellite, all require an exchange of momentum between an energy source and the space vehicle.

Traditionally, any changes to a satellite's orbit have required the use of thrusters and a limited supply of reaction mass. Since no reaction mass will be used in this proposed system, the momentum exchange will take place between the earth and the satellite through the interaction of their respective magnetic fields.

Statement of Purpose

This thesis will analyze the interaction between a magnetic dipole field generated by a current loop around an artificial satellite and a non-uniform expanse of the geomagnetic field. Specifically, it is to quantify the net force available through the interaction of the two fields. This action-at-a-distance force will then be compared to two orbit degradation perturbative forces: atmospheric drag and solar radiation pressure. A comparison will also be made to representative space thrusters currently in use or under consideration. In addition, the force will be evaluated in terms of its potential capability to make minor orbit alterations.

Scope

It is known that satellite attitude and spin rate can be changed by the earth's magnetic field as a result of the torque a magnetic dipole experiences in a uniform magnetic field. This thesis will look at the net force available to act on a satellite in a non-uniform external magnetic field and the possibility of maintaining an artificial satellite's orbital characteristics using geomagnetic field energy in the face of natural decay process or to make minor adjustments to the orbital elements of an artificial satellite.

This research will entail a determination or analysis of:

- The characteristics of the earth's magnetic field
- The interaction between a magnetic dipole and a uniform magnetic field
- The interaction between a magnetic dipole and a non-uniform magnetic field
 - Specifically the net force on a satellite - as a result of a large rigid current loop about the satellite - in the earth's magnetic field
- The effect on a satellite's orbit by the application of such a force

To achieve this, certain assumptions and limitations must be established:

- The system starts out in a stable orbit
 - Only polar orbits will be considered in the derivations
- A non-rotating earth
- The geomagnetic field changes at a predictable rate
- The current carrying loop about the satellite is rigid
- Power requirements can be met
 - No specific hardware will be designed
- The current carrying loop can always be maintained in a given orientation relative to the geomagnetic field

II. LITERATURE REVIEW

Scope

A literature search and review are necessary to resolve several preliminary and fundamental knowledge requirements for this thesis. The four primary categories of search and review are orbital mechanics, magnetostatics, the structure of the geomagnetic field, and present usages of the geomagnetic field.

The topics of orbital mechanics and magnetostatics are well developed and thoroughly covered in textbooks. The specific area of interest in orbital mechanics is the change that takes place in a satellite's orbit by the continuous application of a very small force--rather than the single impulse approximation used with conventional chemical rockets. Small, non impulsive forces are generally dealt with through perturbative techniques. One such technique, with application to this thesis and presented in Appendix A, is Euler's Variation of Parameters.

Within magnetostatics, several preliminary problems need to be understood prior to attempting the computations for this thesis. These are:

- The magnetic dipole generated by a current loop
- The interaction between a magnetic dipole and a uniform magnetic field
- The interaction between a magnetic dipole and a non-uniform magnetic field

The first is covered in most undergraduate textbooks on general physics. The second is covered in textbooks dealing with electromagnetic theory and represents the mathematical concept behind the use of magnetic torques for satellite attitude adjustment (Kaplan, 1976:196f). The last problem is not often addressed but when addressed it is in terms of microscopic particles.

The third category of search and review is the requirement to find an acceptable model of the geomagnetic field. This model will be integrated into the problem of the interaction between a magnetic dipole and a non-uniform magnetic field.

The final area of review is the current use of the geomagnetic field for satellite attitude adjustment. Several related areas that will not be investigated due to simplifying assumptions, but would be necessary for a practical engineering design resolution to the thesis question, include satellite power supply, structural design requirements, satellite attitude stabilization schemes, and launcher constraints.

Orbital Mechanics

Since the action-at-a-distance force that may be derived from the interaction of the satellite magnetic dipole field and the geomagnetic field will be small, the application of the force must be maintained for finite periods and preferably in the most intense region of the geomagnetic

field as possible. This non-impulsive application of force suggests a similarity to low-thrust systems such as ion propulsion (Stuhlinger, 1964:84,89). Low thrust problems must be analyzed using a perturbation approach such as Cowell's, Encke's, or Variation of Parameters (Bate and others, 1971:425). While the optimum impulsive thrust transfer between two coplanar circular orbits is a Hohmann transfer, the optimum infinitesimal thrust transfer is a spiral. Close to the earth the gravitational acceleration is much larger than the thrust acceleration and the spiral will be very tight. A graphic comparison of a Hohmann transfer and a low-thrust transfer is shown in Figure 1.

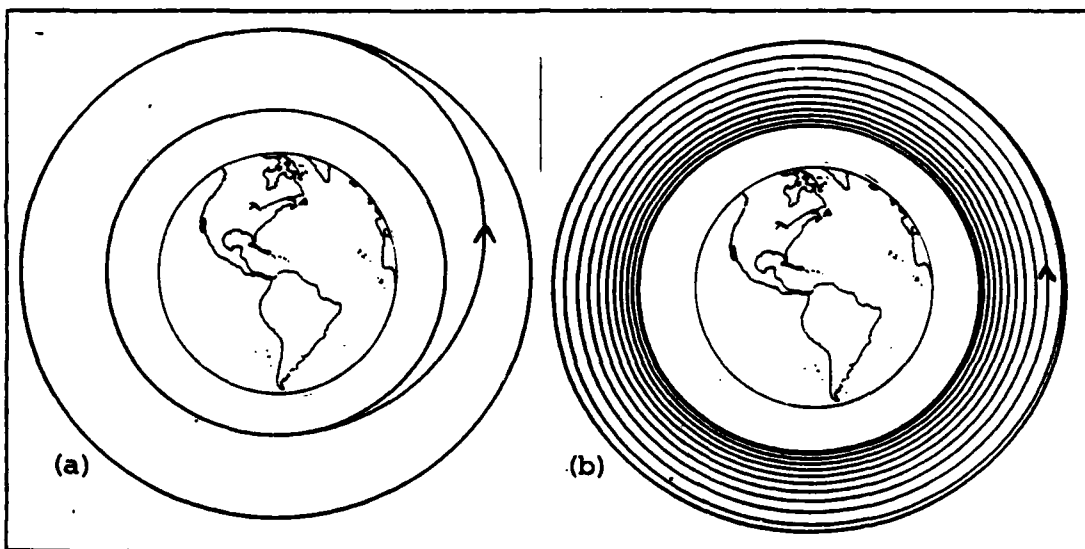


Figure 1. Comparison of a Hohmann Transfer Between Circular Orbit (a) and a Low-Thrust Spiral Transfer Using Infinitesimal Thrust (b)
(Adapted from Edelbaum:117)

Over time the acceleration effects accumulate and the orbit expands more quickly. A general assumption in low-thrust transfer maneuvers is an acceleration that is approximately constant in magnitude and tangential in direction. A review of known solutions to some trajectory optimization problems using impulsive thrust shows that the same orbital transfers are possible using infinitesimal thrust (Edelbaum, 1966:113).

Magnetostatics

Unlike electrostatics, which can point to a unit charge as its fundamental building block, magnetostatics has no magnetic "monopole" that fulfills the same role (Cheston, 1964:149). The fundamental magnetic material is the "motion of charges" (Dart, 1966:66). The motion of electric charges produces a magnetic field. The magnetic field intensity--often referred to as magnetic induction--is a vector field having both direction and magnitude. It is proportional to the current and inversely proportional to the distance from the current (Dart, 1966:68).

When a current is introduced into a magnetic field, there is an interaction. This interaction is felt as a force at right angles to both the current and the field. The magnitude of the force is the product of the external magnetic field intensity and the current (Halliday & Resnick, 1970:559). Figure 2 shows the orientation between the

magnetic field, current, and direction of the force, using the right-hand rule.

If the current forms a circular loop, the magnetic field generated is the same field that would be generated by a magnetic dipole oriented perpendicular to the plane of the circular loop (Halliday & Resnick, 1970:571). If the current-carrying loop is introduced into an external uniform magnetic field, it will experience zero net force and hence no displacement. However, if the dipole moment of the loop is at an angle (θ) to the direction of the external magnetic field, there is a net torque; and the loop will rotate if free to do so as shown in Figure 3. (Halliday & Resnick, 1970:543).

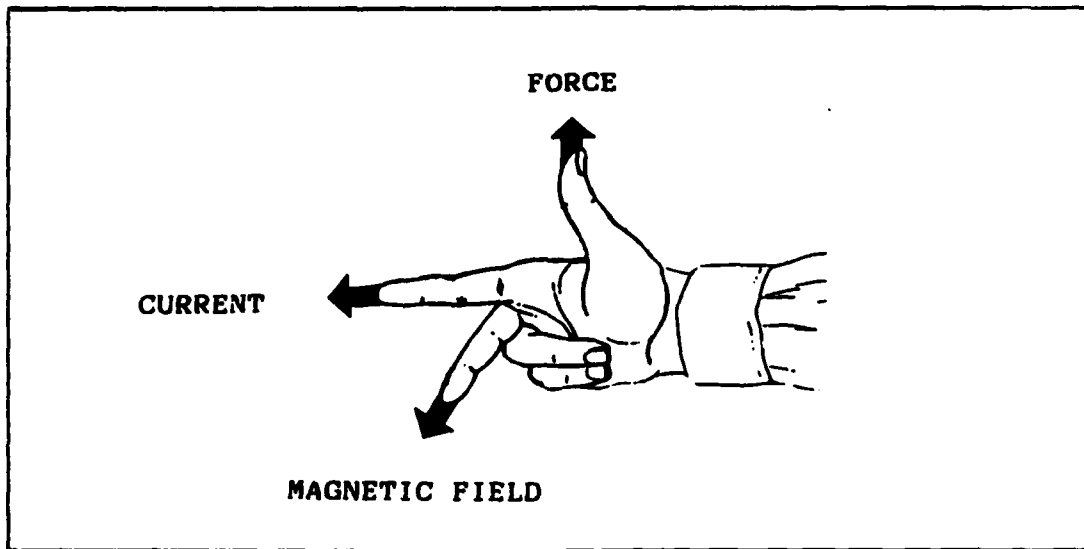


Figure 2. Relative Direction of Magnetic Field, Current & Force

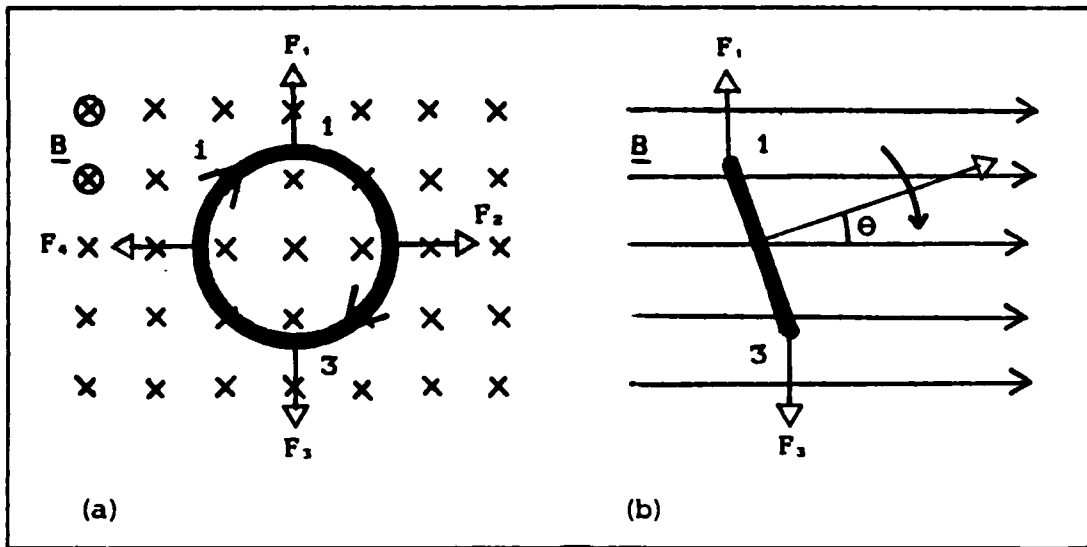


Figure 3. Forces on a Current Loop in a Uniform Magnetic Field (Adapted from Halliday & Resnick:542)

The limited discussion encountered in the literature of a magnetic dipole in a non-uniform magnetic field provided a generalized equation for the force on a localized current distribution in a slowly varying external magnetic field (Jackson, 1967:167). The author's discussion applied the equation to a charged particle--such as might be found in the Van Allen belts surrounding the earth--and provided the basis for the magnetic mirrors discussed in Evans (1985:109). A schematic of the forces acting on a magnetic dipole in a uniform and non-uniform magnetic field are shown in Figure 4.

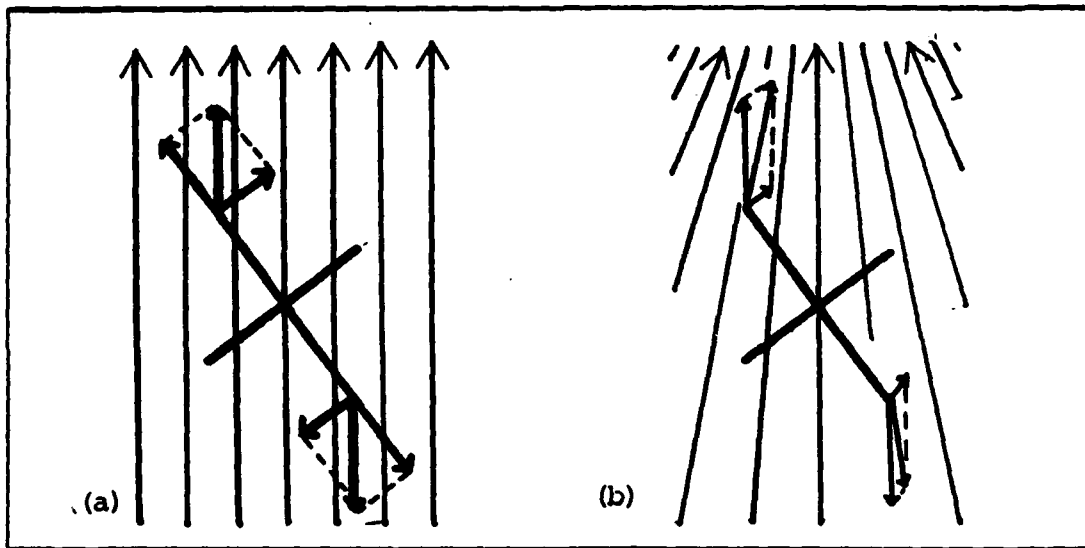


Figure 4. Forces on the Effective Dipole of a Current Loop in a Uniform (a) and a Non-Uniform (b) Magnetic Field

Geomagnetic Models

A magnetic field in free space is usually given as a vector potential; however, it can also be represented in other formats: scalar potentials, orthogonal vectors, Euler potentials or local expansions of the magnetic field around a reference point. All of these additional forms, however, can be converted back to the vector potential format (Stern, 1975:2f).

The geomagnetic field, like any magnetic field, is a vector field, and magnetic field computations can be based on the additive properties of vectors (Klumper, 1982:361). Ideally, the magnetic field at any given point on the surface of the earth or at a satellite's orbit could be calculated by summing up all the contributions from the currents that

influence that point. However, since the earth and its near environment are not a homogeneous mass nor a simple linear current distribution system, the actual vector field is complex and can only be approximated. A common method of approximating a complex function is to use an infinite series expansion. The series can be expanded as necessary to find the dominate terms or to reach a required level of precision. Representations of the geomagnetic field potential are presented, in most cases, as truncated infinite series. The International Geomagnetic Reference Field 1975 (IGRF 1975.0) is used to facilitate comparisons of different models. Represented by a truncated harmonic series of 80 terms, it was constructed by averaging the coefficients of several models.

The simplest representation of the geomagnetic field is the field created by the first term of the expansion. Referred to as the axial dipole model, it is the field created by a dipole whose axis is the earth's rotation axis. This model can be further simplified by the assumption of a perfectly circular orbit (i.e. a perfectly spherical earth).

If the expansion is carried out to three terms, the model now represents the potential of a dipole whose axis is tilted 11.4 degrees to the earth's axis of rotation. This is the oblique or tilted dipole. Further enhancement of the oblique dipole can account for the center of the earth's dipole and the earth's center of mass being separated by up to 500

kilometers (Evans, 1985:93). Various sources and models give displacement distances of 300, 342, 467, and 500 kilometers (Stacy, 1969:129; Alfven, 1963:5; Wertz, 1985:779; Evans, 1985:93). As the radial distance from the earth increases, the dipole approximation becomes increasingly representative of the actual field. However, beyond about two and a half earth radii the dipole nature of the geomagnetic field is distorted by solar activity and other phenomena (Eller, 1983:317).

Models of magnetic fields based on the mathematics of spherical harmonics [related to orthogonal vectors] take the magnetic field at the surface of the earth and expand it radially (Stern, 1975:6). Again, beyond two or three earth radii, the solar wind begins to distort the geomagnetic field and this technique has decreasing utility (Eller, 1983:316f).

Quantitative models of the geomagnetic field tend to fall into two classes: internal models, where the field is due to sources inside the earth and is derived from some type of direct measurements (spherical harmonics and the axial dipole model); and external models that attempt to explain the field by adding the effects of currents above the earth's surface (Mead & Fairfield, 1975:523). As data has become available, models have been--and probably will continue to be--made based on actual satellite measurements of these external currents.

One external model often referenced, and the first to be directly based on field measurements, is the Mead-Fairfield 1972 model. This model was derived from a least-squares fit to 12,616 vector field averages. The measurements were made by four Explorer satellites between 1966 and 1972. The model provides four sets of coefficients to account for "superquiet, quiet, disturbed, and superdisturbed" (Mead & Fairfield, 1975:526) geomagnetic activity. It is considered applicable from five to seventeen earth radii (Fairfield & Mead, 1975:535).

In 1979 a global vector survey of the geomagnetic field was initiated with the launch of MAGSAT. Its mission was to measure the main geomagnetic field as well as the variations caused by crustal anomalies. Due to the sensitivity of the on-board instrumentation, it was also able to investigate other external currents such as the equatorial, auroral zone and polar cap, and high latitude ionosphere and magnetosphere currents. From these measurements a model was developed to account for geomagnetic field perturbations due to various currents in the ionosphere and magnetosphere (Klumpar, 1982:363).

Actual Usages of the Geomagnetic Field

The resultant torque mentioned previously of a magnetic dipole in a uniform magnetic field is the principle by which magnetic torques are employed to adjust satellite attitude.

In the mid-1960's Harold Perkel conceived of a system to control transverse momentum components using the interaction of the geomagnetic field and magnetic torquers on board a satellite. When a magnetic coil's dipole is aligned parallel to the spin axis of a satellite, precession control torques are generated through interaction with the geomagnetic field. By switching the sign of the magnetic coil's magnetic moment at appropriate points in the orbit, the satellite's spin axis can be precessed in any desired direction (Herman, 1977:5). The concept was originally used in the TIROS weather satellite program and later incorporated into the synchronous RCA communications satellites (Kaplan, 1976:196).

This tendency for a magnetic dipole to align itself with an external magnetic field is also one of the primary sources of disturbance torques on satellites (Eller, 1983:316). Vanguard 1 despun from 2.7 to 0.2 revolutions per second in two years due to interaction between on-board magnetic fields and the geomagnetic field (NASA, 1969:2). The Navigation Demonstration Satellite (NDS-2) built by Rockwell for the Global Positioning System (GPS) was originally built to dump momentum with hydrazine thrusters that torque the satellite in the proper direction. However, "Since 1980 the satellites of the GPS system have dumped momentum magnetically, thus avoiding ephemeris disturbance and hydrazine consumption" (Eller, 1983:316). This represents an example of real fuel savings through the use of the geomagnetic field energy.

Conclusion

The calculation of net force acting on a magnetic dipole in a non-uniform magnetic field is representative of the problem of a satellite and its magnetic field operating in earth orbit. The simplest representations of the geomagnetic field are the axial dipole models. These are considered accurate to about three earth radii. For proof of concept and order of magnitude calculations in low to medium earth orbit, a first order spherical harmonic model is a valid approach. For the purposes of this thesis, therefore, an axial model will be used since only low to medium orbits will be considered and the geomagnetic field intensity diminishes as the cube of the distance away from the earth.

III. BACKGROUND THEORY

Introduction

This section will introduce and develop the physics and mathematical equations behind magnetic dipoles and fields and their interaction. Following this discussion will be a restatement of the two-body problem and a brief look at orbital mechanics. The closing section will discuss the equations for geomagnetic field models that exist and are pertinent to this thesis.

Magnetostatics

A starting point for this study is an investigation into the characteristics of magnetic fields. A magnetic field results from the motion of electrically charged particles (such as an electric current in a wire as shown in Figure 5) or the presence of a magnet, and at a given point generates a sideways deflecting force on another electrically charged particle that has an arbitrary initial direction and speed (vector) through that point. Figure 6 shows the curved paths positive and negative electrons take in the presence of a magnetic field as a result of the sideways deflecting force.

The most familiar manifestation of a magnetic field is the torque (twisting or rotating motion) that a small magnet, such as a compass needle, experiences when placed in such a

region. The compass needle will align itself in a north-south direction in the earth's magnetic field or at right angles to a current carrying wire.

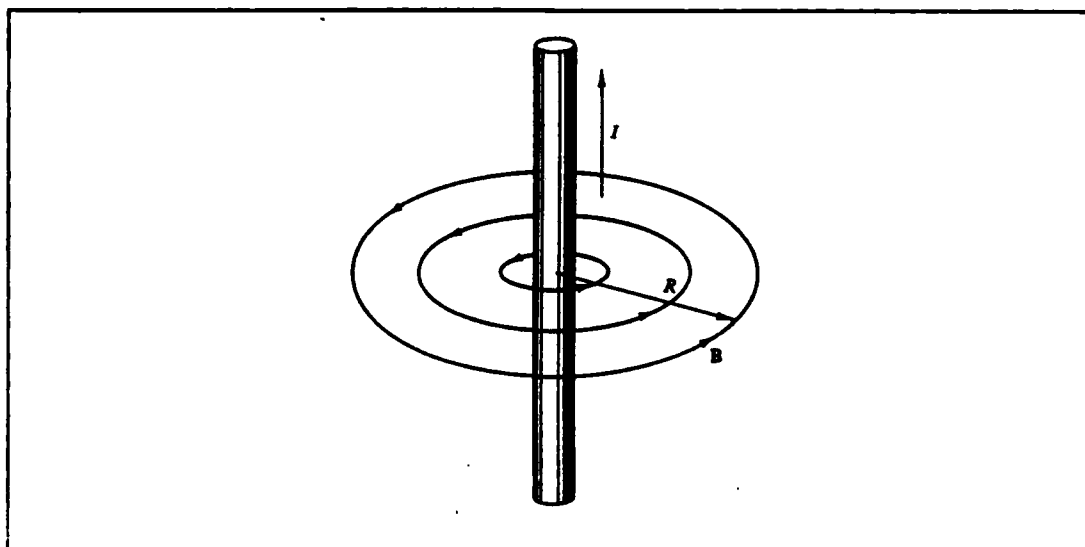


Figure 5. Magnetic Field Around a Current Carrying Wire
(Reprinted from Halliday and Resnick:561)

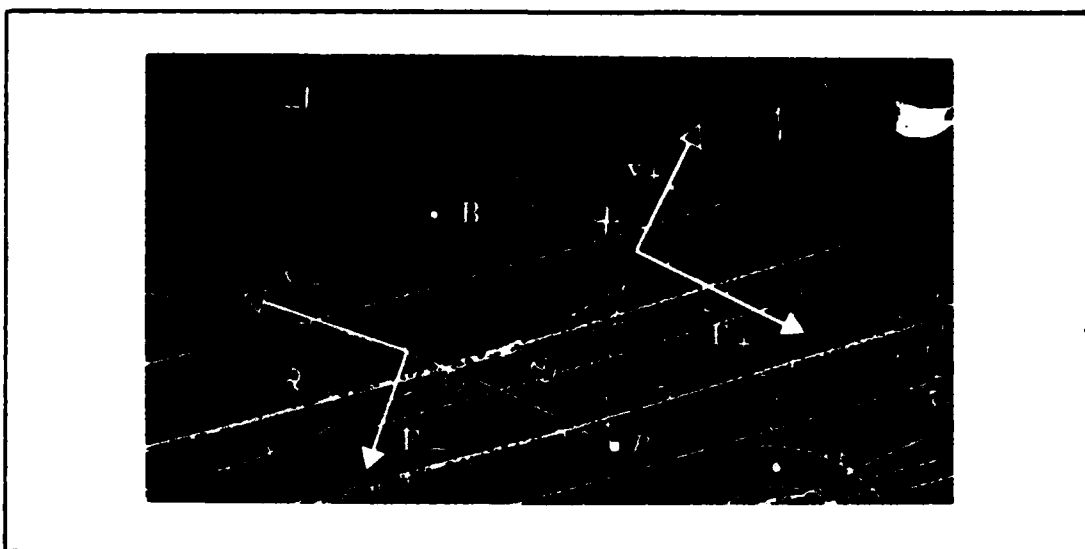


Figure 6. Paths of Positive and Negative Electrons Deflected in Opposite Direction in a Magnetic Field
(Reprinted from Halliday and Resnick:540)

The torque is proportional to the field intensity and to the sine of the angle between the axis of the magnet (the line joining the poles) and the field direction. The direction is determined by the equilibrium position that the north pole of a compass needle will reach when placed in the magnetic field.

Unlike the unit of electrical charge that exists, there is no known magnetic monopole. The simplest magnetic structure is the magnetic dipole, characterized by magnetic dipole moment (μ). The simplest representation is the familiar bar magnet, but magnetic dipoles are also generated by current loops and solenoids.

A mathematical relationship between the magnetic field vector B and the current i is given by Ampere's Law.

$$\oint \mathbf{B} \cdot d\mathbf{L} = \mu_0 i \quad (1)$$

where

\mathbf{B} = magnetic field evaluated around a closed path in space (tesla)
 $d\mathbf{L}$ = displacement vector around a closed path (meters)
 i = current contained within the path of integration (amperes)
 μ_0 = permeability constant

Its usefulness is limited in that the symmetry of the current distribution must be high enough to permit evaluation of the integral such as represented by Figure 7a. Even moderately complex paths can be difficult to integrate (Figure 7b).

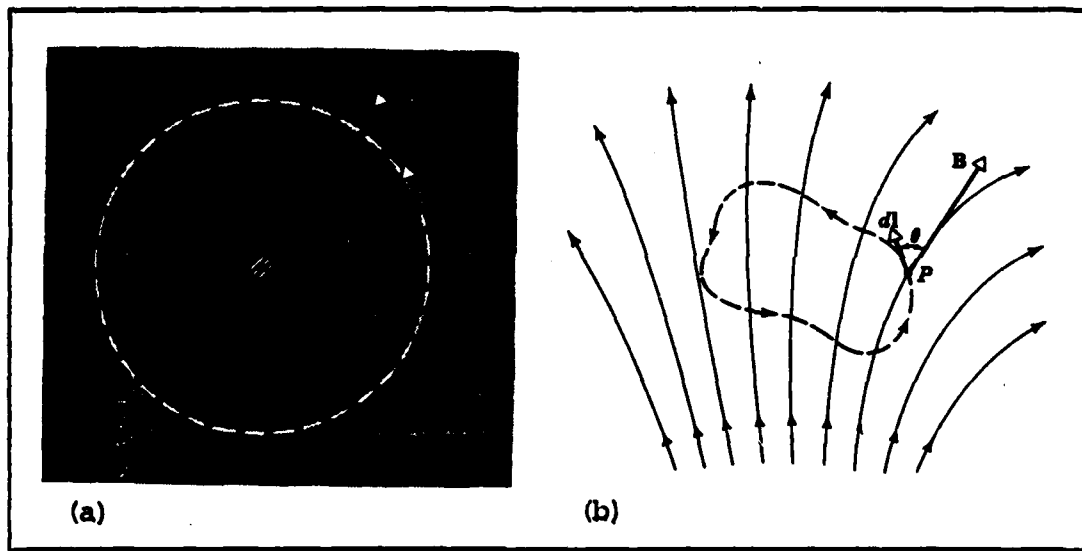


Figure 7. Paths of Integration in a Magnetic Field
(Reprinted from Halliday and Resnick:560)

An example of its application can be found in determining the magnetic field near a long wire.

$$B = \mu_0 i / 2\pi r \quad (2)$$

where r is the radial distance from the wire.

To compute B at any point due to an arbitrary current distribution the Biot-Savart Law states

$$dB = (\mu_0 i / 4\pi) [(dL \times \underline{r}) / r^3] \quad (3a)$$

or

$$dB = (\mu_0 i / 4\pi) [dL \sin(\theta) / r^2] \quad (3b)$$

so that

$$\underline{B} = \int dB \quad (4)$$

In Figure 8, "P" is a point where $d\underline{B}$ is the magnetic field associated with current element dL . The magnitude of $d\underline{B}$ is

given by Eq (3b) and \underline{r} and θ are the displacement vector and direction to "P" from $d\underline{L}$.

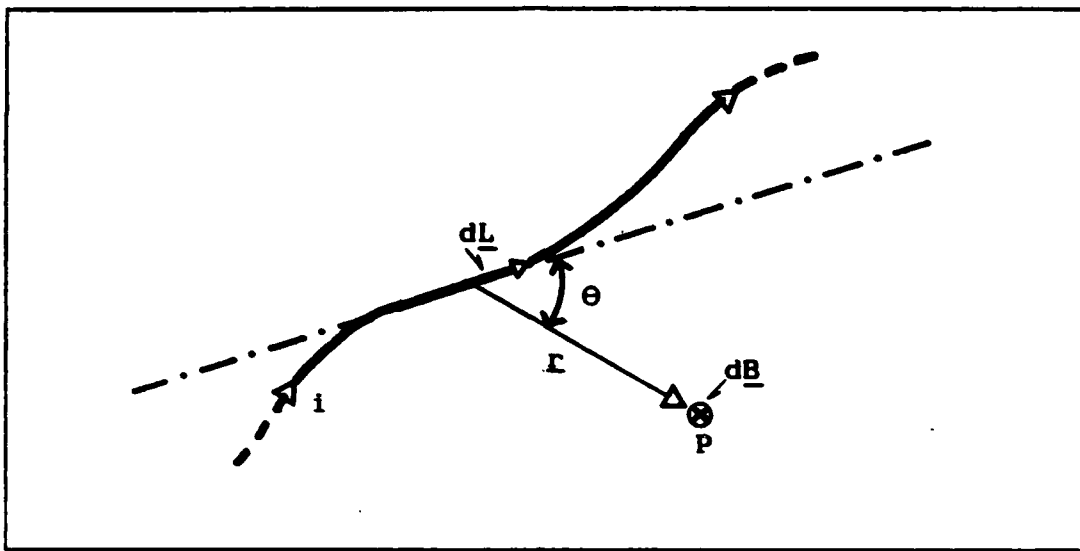


Figure 8. Schematic representation of the Biot-Savart Law where Current Element $d\underline{L}$ Establishes a Magnetic Field Contribution $d\underline{B}$ at "P"
(Adapted from Halliday and Resnick:569)

Therefore a current distribution such as a current loop, generates a magnetic field--the same field that a magnetic dipole aligned perpendicular to the plane of the loop would generate. Application of the Biot-Savart Law gives the magnetic field along the axis of a circular current loop to be

$$B = \mu_0 i R^2 / 2(R^2 + x^2)^{3/2} \quad (5)$$

where

R = radius of the loop

x = distance from the center of the loop to a point along the axis as shown in Figure 9

if $x \gg R$

$$B = \mu_0 i R^2 / 2x^3 \quad (6)$$

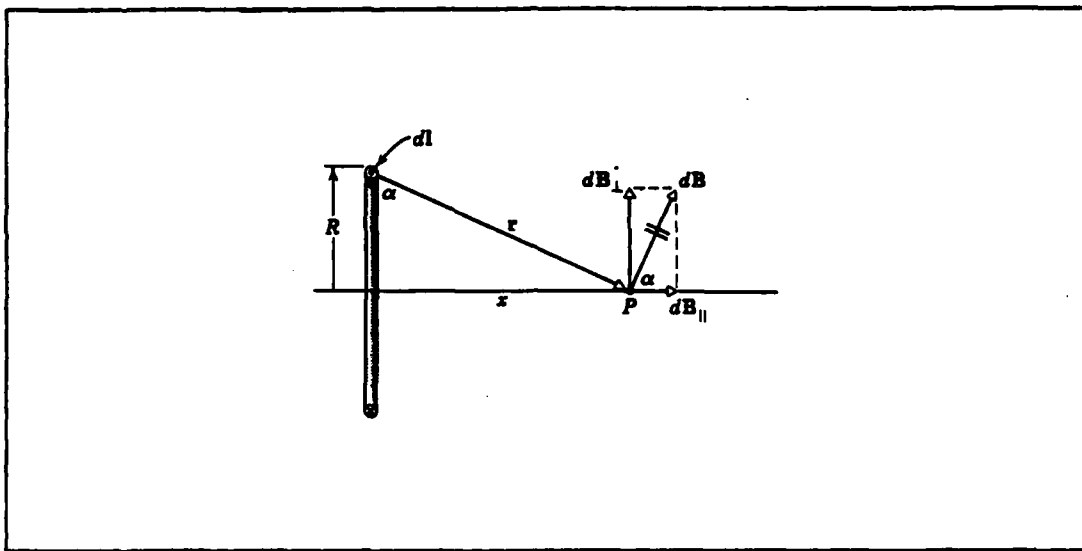


Figure 9. Magnetic Field Along the Axis of a Current Loop
(Reprinted from Halliday and Resnick:570)

Remembering that πR^2 is the area 'A' of the current loop and defining the magnetic dipole (μ) as the current in the loop (i) times the area of the loop (A) times the number of turns of wire in the loop (N) yields:

$$B = \mu_0 N i A / 2\pi x^3 = \mu_0 \mu / 2\pi x^3 \quad (7)$$

Since the geomagnetic field may be approximated by that of a simple magnetic dipole field, the magnetic field around a magnetic dipole is of interest. The equations describing a magnetic dipole field are derived from the magnetic potential in the vicinity of a magnetic dipole.

Referring to Figure 10, let P be a point within the

influence of a simple dipole located at the origin, with P's location described in spherical coordinates (r, θ, ϕ) .

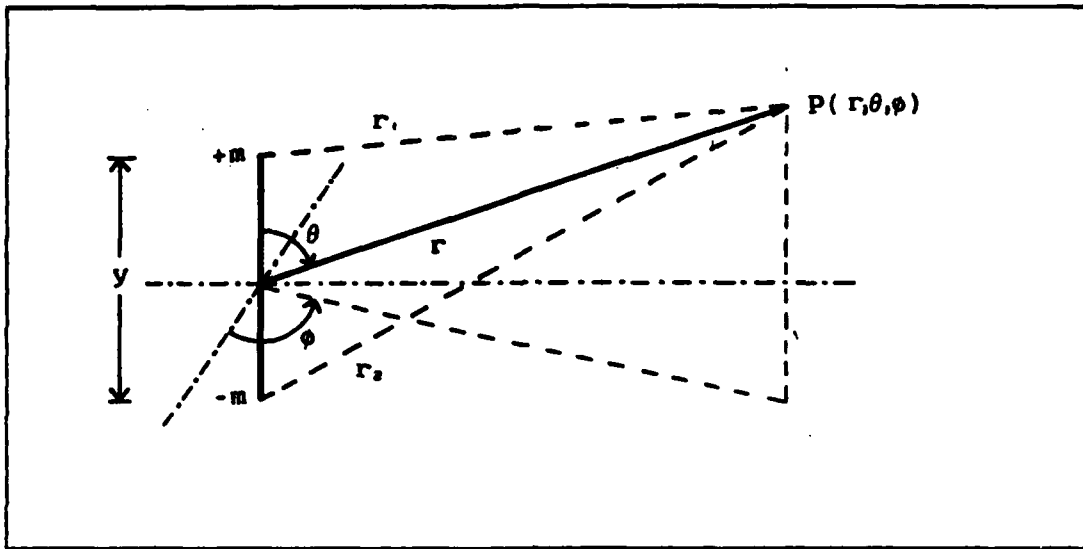


Figure 10. Geometry of Potential Around a Magnetic Dipole

The magnetic moment (μ) is given by the separation (y) between the poles times their pole strength ($\pm m$).

$$\mu = my \quad (8)$$

The potential U at P is then:

$$U = (-m/r_1) + (m/r_2) \quad (9a)$$

$$= -(m)/\{[r^2 + (y/2)^2 - rycos(\theta)]^{1/2}\}$$

$$+(m)/\{[r^2 + (y/2)^2 + rycos(\theta)]^{1/2}\} \quad (9b)$$

If the separation between the poles is much less than the distance to P , that is $y \ll r$, the potential can be given by:

$$U = -mycos(\theta)/r^2 = -\mu cos(\theta)/r^2 \quad (10)$$

The magnetic field at P is then:

$$\mathbf{B} = -\nabla U \quad (11)$$

Letting $\lambda = (\pi/2) - \theta$ be the magnetic latitude, the magnetic field can be defined in terms of its local horizontal (B_λ) and vertical (B_r) components as:

$$B_\lambda = (1/r)(\partial U/\partial \theta) = (2\mu/r^3)(\cos(\lambda)/2) \quad (12)$$

$$B_r = \partial U/\partial r = 2\mu \sin(\lambda)/r^3 \quad (13)$$

The total field strength is then:

$$B = (B_\lambda^2 + B_r^2)^{1/2} = (\mu/r^3)[1 + 3\sin^2(\lambda)]^{1/2} \quad (14)$$

Now consider the affect magnetic fields have on objects within their influence. A positive test charge q_0 moving with velocity v in the presence of a magnetic field B experiences a force given by:

$$\mathbf{F} = q_0 \mathbf{v} \times \mathbf{B} \quad (15)$$

where

F = force (newtons)
 v = velocity of charged particle (meters/second)
 q_0 = charge (coulombs)
 B = magnetic field (tesla)

The units for B stem from this relationship:

$$(nt/coul)/(meter/sec) = weber/meter^2 = tesla$$

$$1 \text{ tesla} = 1 \text{ weber}/\text{meter}^2 = 10000 \text{ gauss}$$

If a charged particle is moving through a region in which both a magnetic field and an electric field exist, the force experienced is given by the Lorentz relation:

$$\mathbf{F} = q_0 \mathbf{E} + q_0 \mathbf{v} \times \mathbf{B} \quad (16)$$

The fact that the magnetic force is always at right angles to the direction of motion means that (for steady magnetic fields) the work done by this force on the particle is zero. ... Thus a steady magnetic field cannot change the kinetic energy of a moving charge; it can only deflect it sideways. (Halliday & Resnick, 1970:539).

Therefore it is reasonable to assume that since a magnetic field exerts a sideways deflecting force on a charged particle it would likewise exert a sideways force on a current carrying wire. This force is given by:

$$\mathbf{F} = i\mathbf{l} \times \mathbf{B} \quad (17)$$

where

\mathbf{l} = displacement vector pointing in the current direction (meters)
 i = current (amperes)
 \mathbf{B} = magnetic field intensity (tesla)

If a current carrying loop is inserted in a uniform magnetic field it will experience a torque (τ) given by:

$$\tau = \mu \times \mathbf{B} \quad (18)$$

with magnitude

$$\tau = \mu B \sin(\theta) \quad (19)$$

with

μ = magnitude of magnetic moment of loop = iA
 θ = angle between vectors μ and \mathbf{B}

The torque will act on every turn of a multiply coiled loop so that

$$\tau = NiAB \sin(\theta) \quad (20)$$

where

N = number of coils in the loop
 i = current (amperes)
 A = area of the loop
 θ = angle between the magnetic field and the magnetic dipole moment of the loop

Two Body Problem

In the two body problem of an earth satellite orbiting about the much larger mass of the earth, the gravitational attraction (F_g) between the two bodies is given by:

$$F_g = -GMm/r^2 \quad (21)$$

where

M = mass of the earth (kg)
m = mass of the satellite (kg)
r = distance of satellite from center of the earth (m)
G = gravitational constant (Nt·m/kg²)

This is based on the following two assumptions:

- 1) The earth and satellite are spherically symmetric so they can be considered as point masses.
- 2) There are no external nor internal forces acting on the pair aside from the gravitational force between them.

If these assumptions are allowed, as well as assuming the satellite is already in a stable orbit, its orbit is governed by the following equations of motion:

$$\ddot{\mathbf{r}} = -G(M+m)\mathbf{r}/r^3 \quad (22)$$

Since, in our system $M \gg m$, it is convenient to say $G(M+m) \approx GM$ and define $GM = k$, then

$$\ddot{\mathbf{r}} + k\mathbf{r}/r^3 = 0 \quad (23)$$

A satellite's position can, in the appropriate coordinate system be defined by a vector \mathbf{r} and its velocity by the vector \mathbf{v} . The moment of momentum (angular momentum per unit mass) vector (\mathbf{h}) is defined by $\mathbf{h} = \mathbf{r} \times \mathbf{v}$ and for a given orbit is constant.

Following the derivation in Thomson and defining $u = 1/r$
the differential equation for the orbit becomes

$$\frac{d^2u}{d\theta^2} + u = k/h^2 \quad (24)$$

This is a second order differential equation requiring two
arbitrary constants in the general solution.

$$u = k/h^2 + C \cos(\theta - \theta_0) \quad (25)$$

With the kinetic energy per unit mass given by $v^2/2$ and the
potential energy per unit mass by $-k/r$ the total energy per
unit mass (E) is:

$$E = (v^2/2) - (k/r) \quad (26)$$

or

$$E = -k/2a \quad (27)$$

where

a = the semi-major axis of a conic section

Choosing $\theta_0 = 0$ in Eq (25), the solution to the orbit equation
can be written

$$u = k/h^2[1 + e \cos(\theta)] \quad (28)$$

where e is the eccentricity for any conic orbit and is given
by:

$$e = (1 + 2Eh^2/k^2)^{1/2} \quad (29)$$

Using the above defined characteristics any orbit can be
fully described in terms of shape, size and orientation by
five independent quantities referred to as "orbital
elements".

These are:

- 1) e = eccentricity
- 2) a = semi-major axis
- 3) i = inclination
- 4) τ = longitude of ascending node
- 5) w = argument of periapsis

If the satellite position must be pinpointed at a particular time a sixth element is also needed.

- 6) T = time of periapsis passage

Other elements are sometimes used such as the semi-latus rectum (p) which is derived from the semi-major axis and the eccentricity, or the longitude of periapsis which is the longitude of the ascending node plus the argument of periapsis. These relationships are shown graphically in Figure 11.

The preceding discussion is dependent upon the two assumptions previously mentioned. To account for the perturbing effects of other masses (sun, moon, planets, etc.) a series of terms must be added to Eq (23) so that we have:

$$\ddot{\mathbf{r}} + (\mathbf{k}\mathbf{r}/\mathbf{r}^3) + \sum_{j=3}^n Gm_j [(\mathbf{r}_{j2}/\mathbf{r}_{j2}^3) - (\mathbf{r}_{j1}/\mathbf{r}_{j1}^3)] = 0 \quad (30)$$

The external accelerations caused by these other masses are small relative to the acceleration by the earth's gravitational field (Bate and others, 1971:11) and for this thesis will be ignored. Other interactions, not considered Keplerian, include perturbations due to the nonspherical earth, atmospheric drag, solar radiation forces, solar wind, eddy currents in the satellite, electromagnetic induction, cosmic dust etc. The interaction of a controlled, internal

current with the earth's magnetic field is the specific perturbation to a satellite's orbit to be considered in this thesis. The variation in the elements that define the orbit over time will be determined based solely on the magnetic field interaction.

Techniques to account for these perturbations include *Variations of Parameters or Elements*, *Cowells Method*, and *Encke's Method*. This thesis will use the Variation of Parameters or Elements as discussed in Bate (1971:396) to outline the procedures to determine the effects of the magnetic field interaction on a satellite's orbital elements.

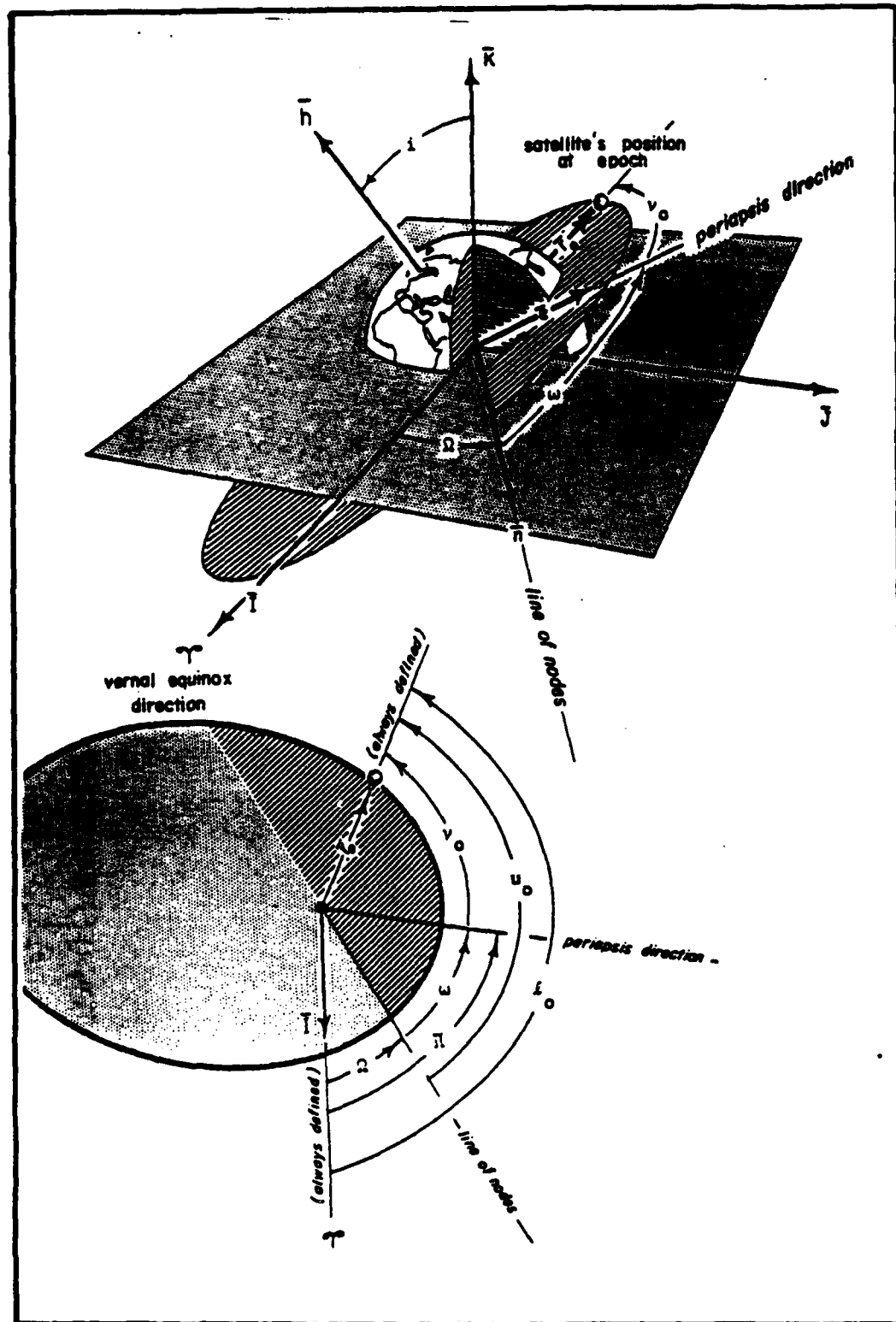


Figure 11. Orbital Elements
(Reprinted from Bate and others:59)

Geomagnetic Field Models

The exact cause of the earth's magnetic field is not known. It is believed to be a result of currents within the earth's core or mantle; the effect of currents located above the surface such as in the ionosphere, or a combination thereof. Gilbert proposed that the earth was a great spherical lodestone. This was discounted due to the lack of lodestone located near the surface. Later Gauss introduced the spherical harmonic expansion of a scalar potential analysis that fit the measurable portions of the geomagnetic field.

Since the field rotates with the earth it is reasonable to assume that most of the field originates from some internal phenomena such as magnetization or a dynamo effect. A field internal to the earth can be described by a solution to a boundary value problem. There are no surface currents on the earth so $\text{curl } \mathbf{B} = 0$ [note: Klumper (1982:361) points out there are external sources, and Mead & Fairfield conclude that $\text{curl } \mathbf{B} \neq 0$ --though by a very small quantity, but Stern (1975:7) points out that internal sources account for 99% of the field]. This lets the field be expressed as the gradient of a scalar potential $\mathbf{B} = -\text{grad } U$. Basic electromagnetic theory says that with no known magnetic monopole, we also have $\text{div } \mathbf{B} = 0$. Combining the last two equations yields Laplace's equation:

$$\text{curl grad } U = 0 \quad (31)$$

The solutions of this equation are well known and can be expressed in terms of functions known as spherical harmonics which are given in units of geocentric coordinates as

$$U(R, \theta, \Phi) = a \sum_{n=1}^{\infty} (a/r)^{n+1} \sum_{m=0}^n [g_n^m \cos(m\Phi) + h_n^m \sin(m\Phi)] P_n^m(\theta) \quad (32)$$

where

a = equatorial radius

g_n^m , h_n^m = Gaussian coefficients (determined empirically by least squares fit of measured values)

(R, θ, Φ) = geocentric distance, coelevation, east longitude from Greenwich which defines a point in space

$P_n^m(\theta)$ = associated Legendre functions

When n=1 the expansion yields a simple dipole, with n=2 the expansion represents a quadrupole, etc. Surface indications such as the Brazilian anomaly (Wertz, 1985:115) indicate the dipole is offset from the earth's center by approximately 474 kilometers (Chapman and Bartels, 1940:12). Therefore the eccentric nature of the dipole is accounted for by the quadrupole expansion. With n=3 the field is that given by an octopole. The IGRF model is a result of n=m=8. The components of the field are given by the respective partial derivatives.

Various analytical attempts have been made to calculate the coefficients but with little success. Field measurements have yielded coefficients empirically through least squares fits. While accurate for the data from which they were calculated, the earth's magnetic pole strength and orientation are subject to secular drift. Consequently the accuracy of the models degrades over time.

Since the dipole field decreases as $1/R^3$ and the quadrupole decreases by $1/R^4$ and higher multipoles decrease even more rapidly, expansions to fewer terms are justified for some calculations. Wertz (1985:119) shows the effects of field truncation and angular errors. As altitude increases the appearance of the geomagnetic field more and more closely resembles that of a magnetic dipole. This thesis is a conceptual analysis attempting to quantify the net force available through the interaction of a satellite magnetic dipole and the geomagnetic field. Instantaneous precise forces are not germane and would only be as accurate as the currency of the coefficients used and will therefore not be attempted. The geomagnetic field will be approximated by an axial dipole model.

IV. DEVELOPMENT

The force that the geomagnetic field exerts on a large orbiting current loop will vary depending on the current the loop is carrying, its radius, and position and orientation relative to the geomagnetic field. A central assumption of this thesis is that the current loop can be maintained in any desired orientation relative to the earth and the geomagnetic field throughout its orbit.

Four orientations will be discussed and analyzed. Case I will align the satellite's magnetic dipole parallel to the radial component of the geomagnetic field, so that the plane of the current loop is parallel to the earth's surface. Case II will look at the force as a result of an alignment of the current loop's dipole with the theta component of the geomagnetic field, so that the current loop is always perpendicular to the earth's surface. Case III will investigate the force as a result of alignment of the current loop's dipole with the instantaneous geomagnetic field at each point in the satellite's orbit. In Case IV the satellite will maintain a constant inertial orientation. This fourth orientation can be generalized to any arbitrary orientation. Figure 12 shows the four cases and their orientation with respect to the earth, each other and the components of the geomagnetic field.

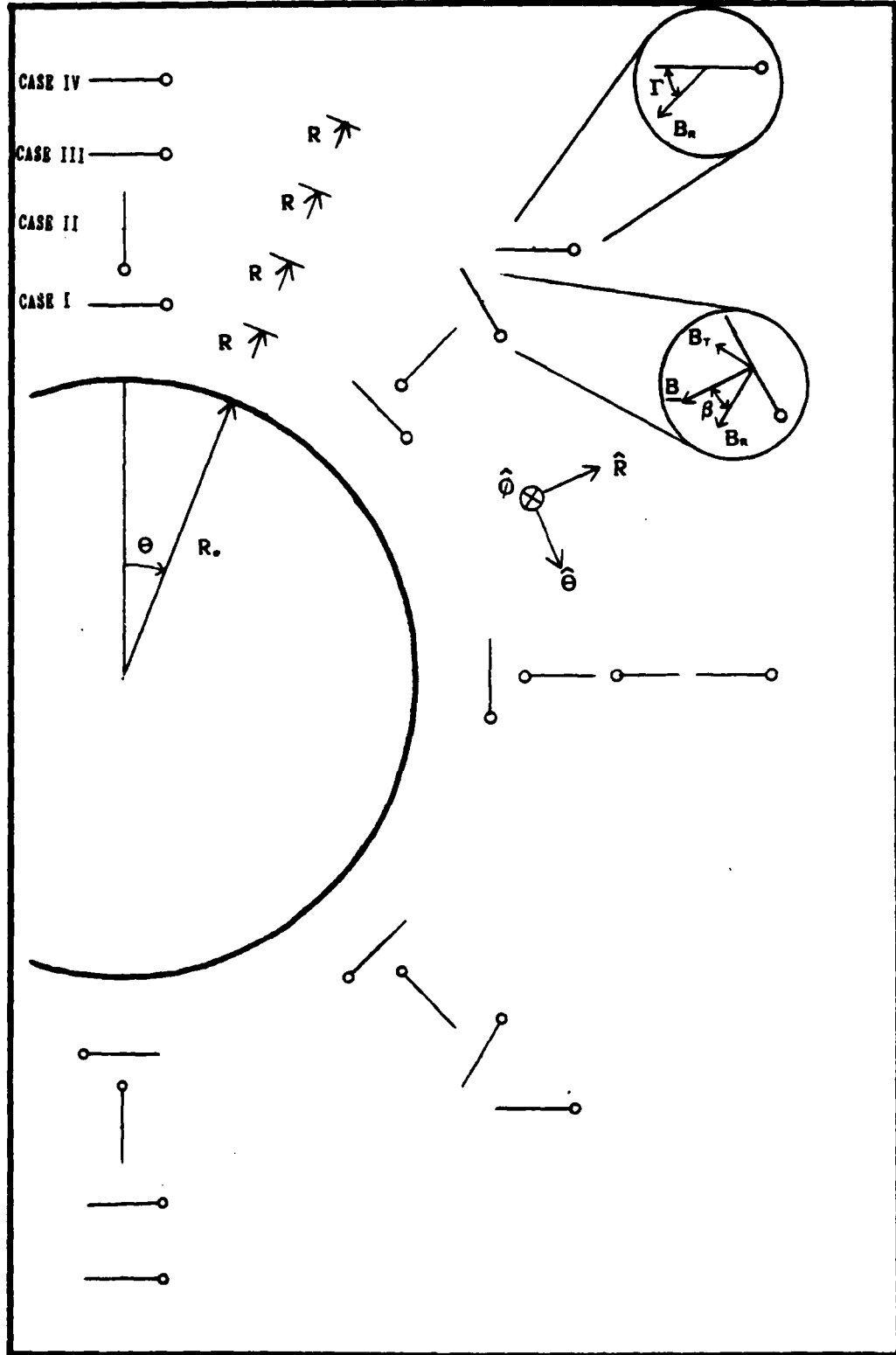


Figure 12. Four Orientations of the Current Loop Relative to the Earth and Each Other

Method Used In Derivation

The equations representing the force on the current loop will now be derived as functions of the radial distance from the center of the earth and the co-latitude position. While the geomagnetic field is strongest and a greater gradient exists near the poles, the net effective force is not necessarily greatest at the poles. However, since the force will act in the theta or radial direction the interactive force is most advantageously applied to a satellite in a polar orbit.

The force on each section of the current loop is due to the interaction between the current displacement vector for that section and the geomagnetic field vector acting on that section. The direction of the force is perpendicular to both the current vector and geomagnetic field. This implies that the radially directed component of the force (F_R) is a result of the theta component of the geomagnetic field (B_θ). Likewise, the force component in the theta direction (F_θ) is due to the radial component of the geomagnetic field (B_R). The force in the phi (longitude) direction (F_ϕ) will be shown to be zero.

It is the force on the loop itself that is of interest, but the position of the loop will be defined by the location of its center only, that is, a radial distance (R_0) and co-latitude theta (θ_0). The geomagnetic field does not change with the longitude, therefore the longitudinal position of

the center (Φ_0) does not need to be considered in this derivation since it does not contribute to the solution. The position of the center of the loop (R_0, θ_0, Φ_0) will be referred to by position vector R_0 . The magnetic field interacting with the loop at location R is the magnetic field at the radius, r , from the center of the loop. This is given by the gradient of the magnetic field at the center of the loop dotted into the distance (r), given by Eq (34) below, to the current carrying wire.

The equation for the magnetic field of interest at a point (R, θ, Φ) can be expressed as:

$$\underline{B}(R, \theta, \Phi) = \underline{B}(R_0, \theta_0, \Phi_0) + (\text{del } \underline{B}) \cdot \underline{r} \quad (33)$$

where

$$\underline{r} = (R - R_0)\hat{\underline{R}} + (\theta - \theta_0)\hat{\underline{\theta}} + (\Phi - \Phi_0)\hat{\underline{\Phi}} \quad (34)$$

also

$$\underline{B}(R, \theta, \Phi) = B_R(R, \theta, \Phi)\hat{\underline{R}} + B_\theta(R, \theta, \Phi)\hat{\underline{\theta}} + B_\Phi(R, \theta, \Phi)\hat{\underline{\Phi}} \quad (35)$$

Expanding each scalar component:

$$B_R(R, \theta, \Phi) = B_R(R_0, \theta_0, \Phi_0) + \partial B_R / \partial R |_{\theta_0, \Phi_0} \Delta R + \partial B_R / \partial \theta |_{R_0, \Phi_0} \Delta \theta + \partial B_R / \partial \Phi |_{R_0, \theta_0} \Delta \Phi \quad (36)$$

$$B_\theta(R, \theta, \Phi) = B_\theta(R_0, \theta_0, \Phi_0) + \partial B_\theta / \partial R |_{\theta_0, \Phi_0} \Delta R + \partial B_\theta / \partial \theta |_{R_0, \Phi_0} \Delta \theta + \partial B_\theta / \partial \Phi |_{R_0, \theta_0} \Delta \Phi \quad (37)$$

$$B_\Phi(R, \theta, \Phi) = B_\Phi(R_0, \theta_0, \Phi_0) + \partial B_\Phi / \partial R |_{\theta_0, \Phi_0} \Delta R + \partial B_\Phi / \partial \theta |_{R_0, \Phi_0} \Delta \theta + \partial B_\Phi / \partial \Phi |_{R_0, \theta_0} \Delta \Phi \quad (38)$$

where $\Delta R = R - R_0$ and $\Delta \theta = \theta - \theta_0$.

However $B_\Phi = 0$, which eliminates those four terms from consideration. Also B_R and B_θ do not contain a phi term which eliminates two additional terms. Finally the terms for the field at the center of the loop will integrate to a zero

net force--since they represent the loop in a uniform magnetic field--and need not be considered.

The remaining radial and theta components of the magnetic field and their partial derivatives are expressed and evaluated as follows:

$$\frac{\partial B_r}{\partial R} = \frac{\partial}{\partial R}[-2(Re/R)^3 g^0 \cos(\theta)] = 6Re^3 g^0 \cos(\theta)/R^4 \quad (39)$$

$$\frac{\partial B_r}{\partial \theta} = \frac{\partial}{\partial \theta}[-2(Re/R)^3 g^0 \cos(\theta)] = 2(Re/R)^3 g^0 \sin(\theta) \quad (40)$$

$$\frac{\partial B_t}{\partial R} = \frac{\partial}{\partial R}[-(Re/R)^3 g^0 \sin(\theta)] = 3Re^3 g^0 \sin(\theta)/R^4 \quad (41)$$

$$\frac{\partial B_t}{\partial \theta} = \frac{\partial}{\partial \theta}[-(Re/R)^3 g^0 \sin(\theta)] = -(Re/R)^3 g^0 \cos(\theta) \quad (42)$$

where

Re = earth's radius

R = orbit radius

g^0 = first Gaussian coefficient

θ = colatitude

The evaluation of the gradient still requires the determination of ΔR and $\Delta \theta$. From Figures 13-16 these can be seen to be $\pm r \sin(\Omega) \sin(\text{defined orientation angle})$ and $\pm (r/R) \sin(\Omega) \cos(\text{defined orientation angle})$ respectively. In addition dL can be seen to be $rd\Omega$.

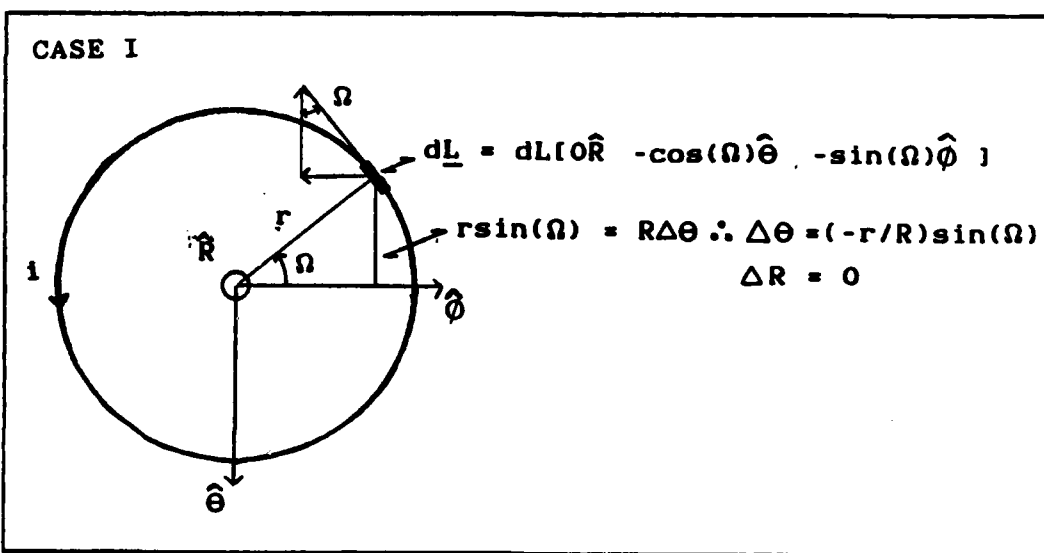


Figure 13. Case I: Current Loop and Orientation Relative to the Geomagnetic Field and Definitions of $d\mathbf{L}$, ΔR and $\Delta\theta$.

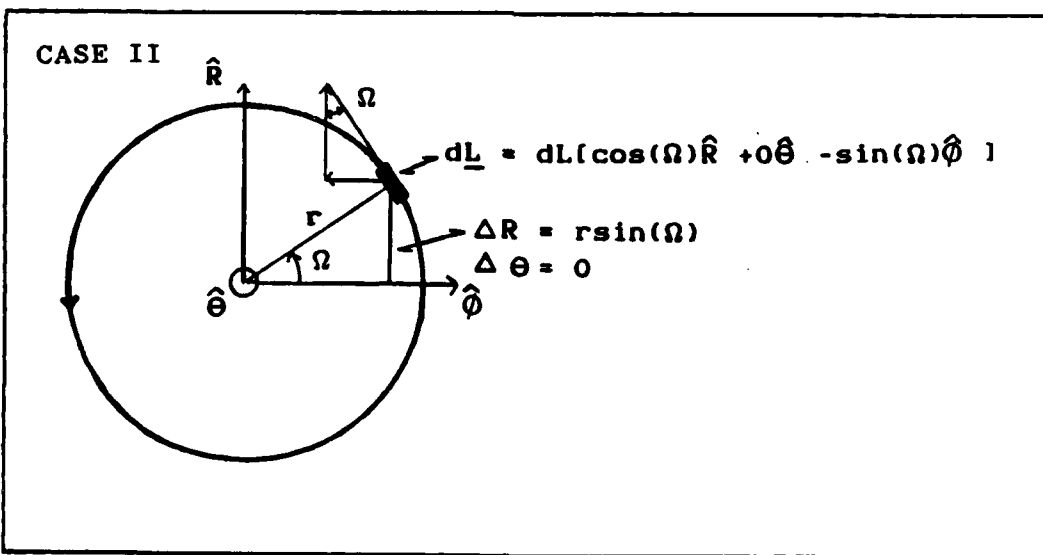


Figure 14. Case II: Current Loop and Orientation Relative to the Geomagnetic Field and Definitions of $d\mathbf{L}$, ΔR and $\Delta\theta$.

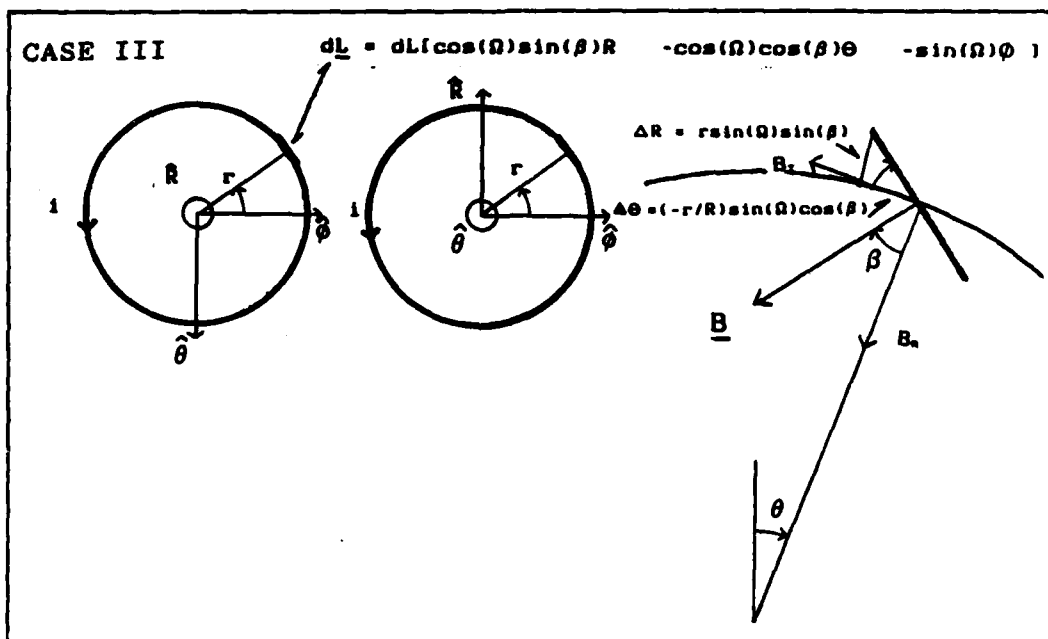


Figure 15. Case III: Current Loop and Orientation Relative to the Geomagnetic Field and Definitions of $d\mathbf{L}$, ΔR and $\Delta\theta$.

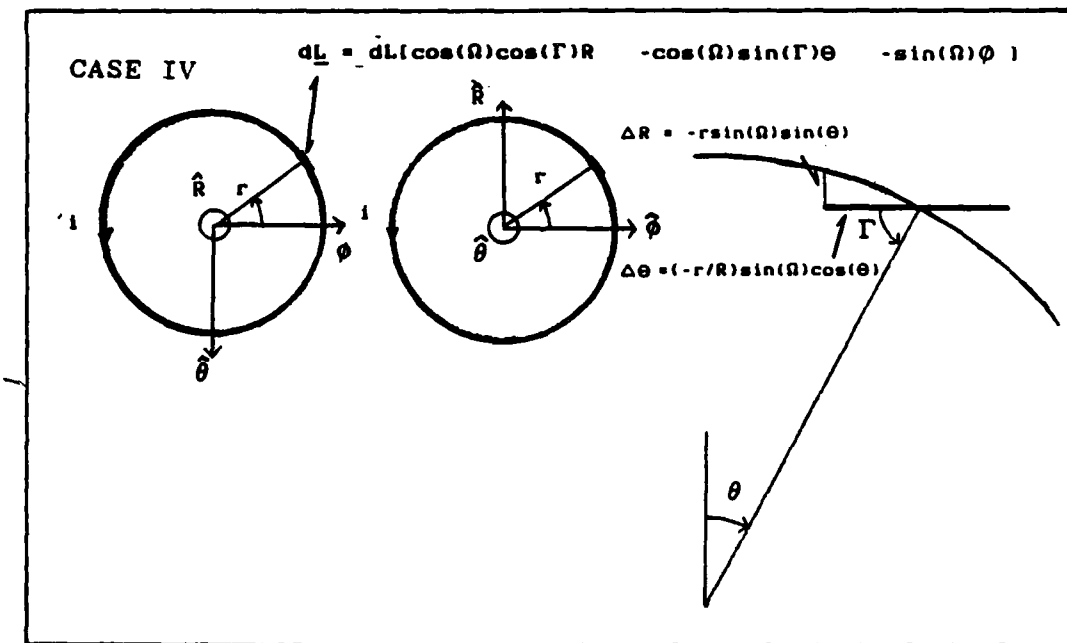


Figure 16. Case IV: Current Loop and Orientation Relative to the Geomagnetic Field and Definitions for $d\mathbf{L}$, ΔR , and $\Delta\theta$.

Case I: Loop Parallel to Earth's Surface

When the current loop is aligned with its dipole parallel to the radial component of the geomagnetic field, the current loop's orientation is approximately parallel to the earth's surface. The periphery of the loop is assumed to be at the same distance as the center of the loop from the center of the earth. At a point exactly over the geomagnetic pole the radial component of the geomagnetic field yields a force that is directed radially with respect to the current loop and is therefore self-cancelling. Also, exactly over the magnetic pole the B_r component is zero. At equal, small distances away in all directions parallel to the geomagnetic equatorial plane the magnitude of B_r is small and equal at all points on the loop. The B_r component of the geomagnetic fields provides a force in the positive or negative radial direction (depending on the direction of current flow) with respect to the center of the earth. The B_r component at a location exactly centered over the pole therefore provides a net effective force of $2\pi riB_r$ acting on the satellite. As the satellite moves away from the pole the net effective force will have contributions from both components of the geomagnetic field.

The following derivation of the components of the force on the current loop makes the assumption that for each dL of the current loop the component of the geomagnetic field is parallel but of slightly different magnitude. Exactly over

the pole and for distances close to the pole this is not precisely correct. However, the convergence of components of \mathbf{B} at the extreme points of the loop (1000 meter radius current loop in a 600 kilometer orbit) is less than 0.5 degrees at one degree from the pole and less than 5 degrees when 0.1 degree from the pole. Figures 12 and 13 define the components of the geomagnetic field, orientation of the current loop and axes of the coordinate systems for the current loop and the geomagnetic field.

The force on each infinitesimal of the current loop is

$$d\mathbf{F} = i dL \times \mathbf{B} \quad (43)$$

The vector dL can take one of two forms depending on the direction of current flow in the loop. For purposes of this derivation the current will be considered in a clockwise direction when the satellite is viewed from the earth's center.

The infinitesimal force expressed in determinant form is then

$$d\mathbf{F} = i dL \begin{vmatrix} \hat{\mathbf{R}} & \hat{\theta} & \hat{\phi} \\ 0 & -\cos(\Omega) & -\sin(\Omega) \\ B_R & B_\theta & 0 \end{vmatrix}$$

Therefore,

$$d\mathbf{F} = idL[B_\theta \sin(\Omega)\hat{\mathbf{R}} - B_R \sin(\Omega)\hat{\theta} + B_R \cos(\Omega)\hat{\phi}] \quad (44)$$

Each component of the force is given by the respective component in the preceding equation. The force in the radial direction (F_R) is given by:

$$F_R = \int dF_R \hat{\mathbf{R}} = \int ir \sin(\Omega) d\Omega B_R \quad (45)$$

Substituting Eq (37) for B_r , and noting from Figure 13 that

$$\Delta R = 0 \quad (46)$$

and

$$\Delta\theta = -(r/R)\sin(\Omega) \quad (47)$$

the integral becomes:

$$\int ir[-(Re/R)^3 g^0 \cos(\theta)](-r/R)\sin(\Omega)\sin(\Omega)d\Omega \quad (48)$$

R and θ define the location of the loop and i , r , g^0 , and Re are constants. Consolidating and pulling the constants out of the integral yields:

$$ir^2 Re^3 g^0 \cos(\theta)/R^4 \int \sin^2(\Omega)d\Omega \quad (49)$$

When the integral is evaluated around the loop (2π) the force in the radial direction is:

$$F_{R1} = i\pi r^2 Re^3 g^0 \cos(\theta)/R^4 \quad (50)$$

The force in the theta direction (F_θ) is given by:

$$F_\theta = \int dF_\theta \theta = \int -irs\in(\Omega)d\Omega B_r \quad (51)$$

Substituting Eq (36) for B_r and recalling Eq (46) and (47) the integral becomes:

$$\int -ir^2(Re/R)^3 g^0 \sin(\theta)(-r/R)\sin(\Omega)\sin(\Omega)d\Omega \quad (52)$$

Pulling the constants out of the integral yields:

$$2ir^2 Re^3 g^0 \sin(\theta)/R^4 \int \sin^2(\Omega)d\Omega \quad (53)$$

When evaluated around the loop the force in the theta direction is:

$$F_{\theta1} = 2(i\pi r^2 g^0 Re^3 / R^4) \sin(\theta) \quad (54)$$

The force in phi direction (F_ϕ) should be zero and the following evaluation confirms this. The force is represented by:

$$F_\phi = \int dF_\phi \hat{\Phi} = \int i r \cos(\Omega) d\Omega B_R \quad (55)$$

Substituting Eq (36) for B_R and recalling Eq (46) and (47) the integral becomes:

$$\int i r^2 (R_e/R)^3 g^0 \sin(\theta) (-r/R) \cos(\Omega) \sin(\Omega) d\Omega \quad (56)$$

Consolidating terms and pulling constants to the left of the integral yields:

$$-(2ir^2 g^0 R_e^3 / R^4) \sin(\theta) \int \cos(\Omega) \sin(\Omega) d\Omega \quad (57)$$

The integral, when evaluated around the loop (2π) yields zero, leaving a zero force in the phi direction.

The total force is then:

$$F_I = (F_{R,I}^2 + F_{T,I}^2)^{1/2} = i\pi r^2 g^0 R_e^3 / R^4 [1 + 3\sin^2(\theta)]^{1/2} \quad (58)$$

The direction of the force is dependent on the direction of the current flow. When the current is clockwise as seen from the center of the earth, then the radial, theta, and total forces vary with co-latitude as shown in Figure 17. The magnitudes are representative of a current loop carrying 10 amps and a radius of 1000 meters.

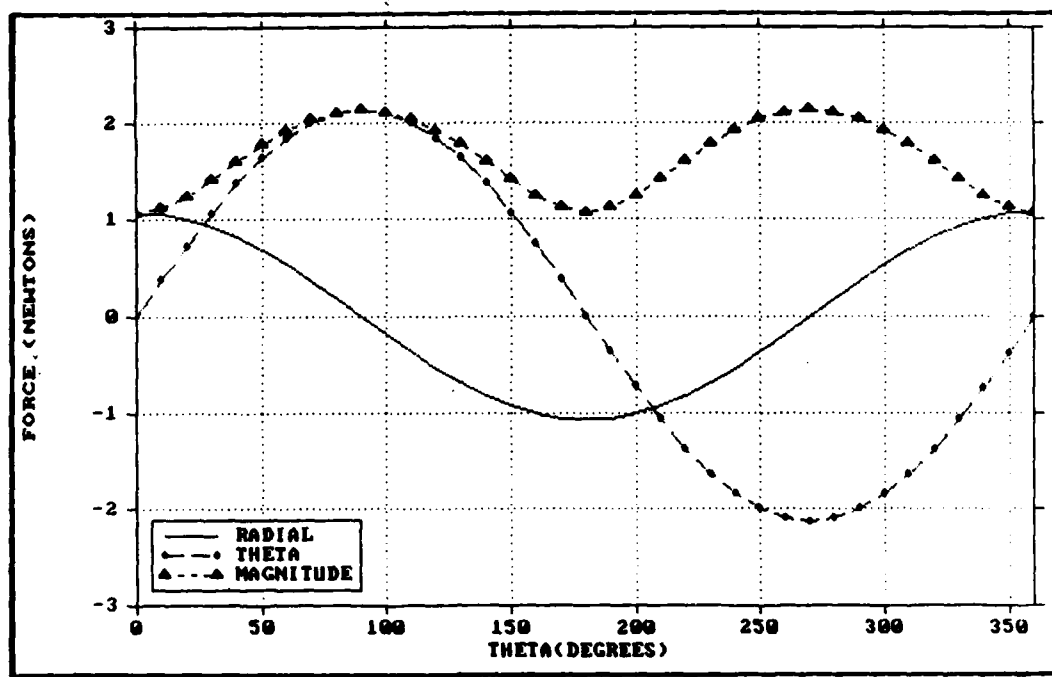


Figure 17. Magnetic Forces for Case I (600 Kilometer Orbit)

Case II: Loop Perpendicular to Earth's Surface

With the current loop aligned with its dipole parallel to the theta component of the geomagnetic field (B_θ), the current loop will maintain an orientation perpendicular to the earth's surface as shown in Figure 12. Directly over the pole ($B_\theta = 0$) the net force can be directed entirely in the direction of orbital motion by proper selection of the direction of current flow. As the satellite moves away from the pole, components of force are added in the radial direction. Again, for the following derivation, the assumption is made that the B_θ or B_ϕ components at the extremities of the current loop are parallel. Figures 12 and 14 define for Case II the components of the geomagnetic field, orientation of the current loop, and axes of the coordinate systems for the current loop and the geomagnetic field.

The force on the current loop is again given by Eq (43). However, since the loop now lies in the $R-\Phi$ plane, $d\mathbf{L}$ is given by $d\mathbf{L}[\cos(\Omega)\hat{\mathbf{R}} \quad 0\hat{\mathbf{\theta}} \quad -\sin(\Omega)\hat{\mathbf{\Phi}}]$. Expanding the cross product, the infinitesimal force is

$$d\mathbf{F} = i d\mathbf{L} [B_\theta \sin(\Omega)\hat{\mathbf{R}} - B_\theta \sin(\Omega)\hat{\mathbf{\theta}} + B_\theta \cos(\Omega)\hat{\mathbf{\Phi}}] \quad (59)$$

The procedure for determining the force in the radial and theta directions is the same as shown in Case I.

Substituting Eq (37) for B_r and noting from Figure 14 that

$$\Delta\theta = 0 \quad (60)$$

and

$$\Delta R = r\sin(\Omega) \quad (61)$$

the force in the radial direction is:

$$F_{RII} = (i\pi r^2 g^0 R e^3 / R^4) 3\sin(\theta) \quad (62)$$

Which is zero over the pole ($\theta = 0$) and a maximum at the equator as expected.

Substituting Eq (36) for B_θ and recalling Eq (60) and (61) the force in the theta direction is:

$$F_{TII} = -6\cos(\theta)(i\pi r^2 g^0 R e^3 / R^4) \quad (63)$$

The force in the phi direction is again zero because the integral ultimately contains the $\sin(\Omega)\cos(\Omega)$ term.

The total force acting on this orientation is then

$$F_{II} = (F_R^2 + F_T^2)^{1/2} = 3i\pi r^2 g^0 R e^3 / R^4 [1+3\cos^2(\theta)]^{1/2} \quad (64)$$

Figure 18 shows the forces for Case II as they vary with co-latitude. The magnitudes are again representative of a current loop carrying 10 amps with a 1000 meter radius.

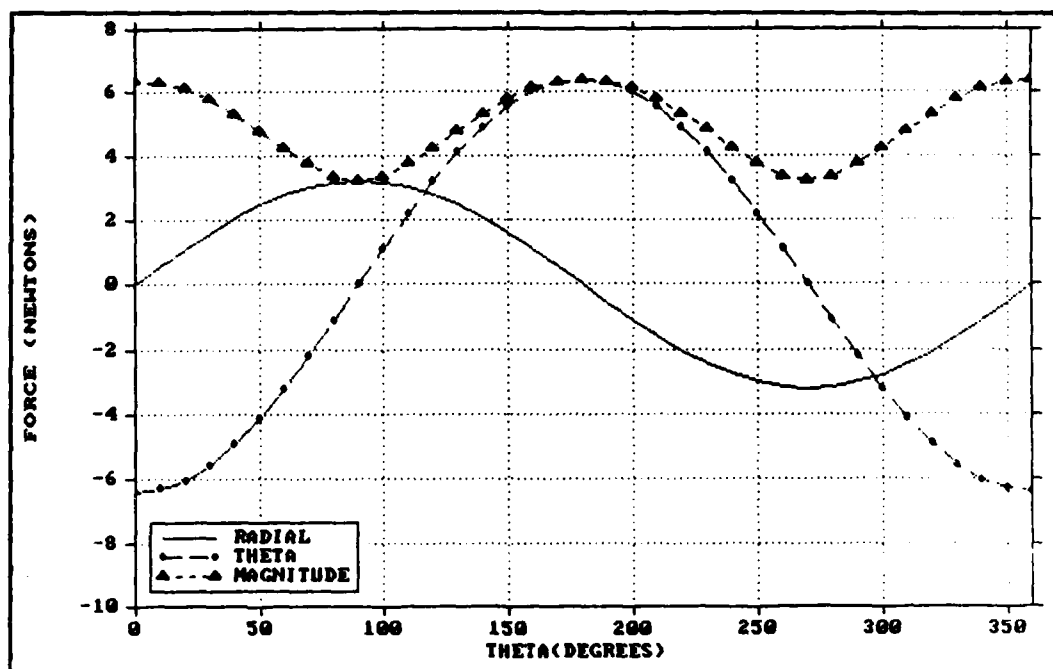


Figure 18. Magnetic Forces for Case II (600 Kilometer Orbit)

Case III: Loop Dipole Parallel to Geomagnetic Field Vector

For this third case the current loop is constantly changing its orientation with respect to the earth's surface so as to maintain a constant orientation relative to the instantaneous geomagnetic field vector. The added complexity of this case is offset by the merit this orientation has in minimizing the torque experienced by the current loop. As can be seen in Figure 12 the satellite will make two complete rotations about its center of mass for each orbit about the earth. Identical to Case I when directly over the pole, it becomes Case II when at the equator.

The determination of the force again assumes that the component of the geomagnetic field affecting each section of the loop is parallel for every section of the loop. The angle beta (β) defines the orientation of the loop at any given point in its orbit and, as can be seen in Figure 12 and 15, is the angle between the current loop's magnetic dipole (or instantaneous geomagnetic field vector) and the radius vector to the current loop from the center of the earth.

The force on the loop is again given by Eq (43) and the expansion of the cross product is:

$$\begin{aligned} d\mathbf{F} = i \, dL \{ & B_r \sin(\Omega) \hat{\mathbf{R}} - B_\theta \sin(\Omega) \hat{\mathbf{\theta}} \\ & + [B_r \cos(\Omega) \sin(\beta) + B_\theta \cos(\Omega) \cos(\beta)] \hat{\mathbf{\phi}} \} \end{aligned} \quad (65)$$

The force in the radial direction is given by Eq (45)

$$F_R = \int dF_R \hat{\mathbf{R}} = \int i r \sin(\Omega) d\Omega B_r \quad (45)$$

Substituting Eq (37) for B_r and noting from Figure 15 that

$$\Delta R = r \sin(\Omega) \sin(\beta) \quad (66)$$

and

$$\Delta\theta = -(r/R) \sin(\Omega) \cos(\beta) \quad (67)$$

the integral becomes:

$$\int i r \sin(\Omega) d\Omega \{ 3(Re^3/R^4) g^0 \sin(\theta) [r \sin(\Omega) \sin(\beta)] \\ - (Re/R)^3 g^0 \cos(\theta) (-r/R) \sin(\Omega) \cos(\beta) \} \quad (68)$$

Forming two integrals, consolidating terms and pulling the constants out of the integrand yields:

$$3 \sin(\theta) \sin(\beta) (ir^2 g^0 Re^3 / R^4) \int \sin^2(\Omega) d\Omega \\ + \cos(\theta) \cos(\beta) (ir^2 g^0 Re^3 / R^4) \int \sin^2(\Omega) d\Omega \quad (69)$$

Evaluating the integrals around the current loop yields a force in the radial direction of

$$F_{R111} = (i \pi r^2 g^0 Re^3 / R^4) [3 \sin(\theta) \sin(\beta) + \cos(\theta) \cos(\beta)] \quad (70)$$

Which gives the same results as Case I over the pole and Case II over the equator.

The force in the theta direction is again given by Eq (51):

$$F_\theta = \int dF_\theta \hat{\theta} = \int -i r \sin(\Omega) d\Omega B_\theta \quad (51)$$

Substituting Eq (36) for B_θ and recalling Eq (66) and (67) the integral becomes:

$$\int -i r \sin(\Omega) d\Omega \{ 6(Re^3/R^4) g^0 \cos(\theta) [r \sin(\Omega) \sin(\beta)] \\ + 2(Re/R)^3 g^0 \sin(\theta) [(-r/R) \sin(\Omega) \cos(\beta)] \} \quad (71)$$

Forming two integrals, consolidating terms and pulling the constants outside the integrals yields:

$$\begin{aligned} & -6\cos(\theta)\sin(\beta)(ir^2g^0Re^3/R^4) \int \sin^2(\Omega)d\Omega \\ & + 2\sin(\theta)\cos(\beta)(ir^2g^0Re^3/R^4) \int \sin^2(\Omega)d\Omega \quad (72) \end{aligned}$$

Evaluating the integrals around the current loop gives the force in the theta direction as

$$F_{\text{r III}} = 2(ir^2g^0Re^3/R^4)[\sin(\theta)\cos(\beta) - 3\cos(\theta)\sin(\beta)] \quad (73)$$

Which again gives the same result as Case I over the pole and Case II over the equator.

The force in the phi (Φ) direction again equals zero because each integral contains a $\sin(\Omega)\cos(\Omega)$ term. The total force is given by

$$F_{\text{III}} = (F_{\text{r III}}^2 + F_{\text{t III}}^2)^{1/2} \quad (74)$$

The radial, theta, and total force for Case III are shown in Figure 19 for the same representative current loop as in Case I.

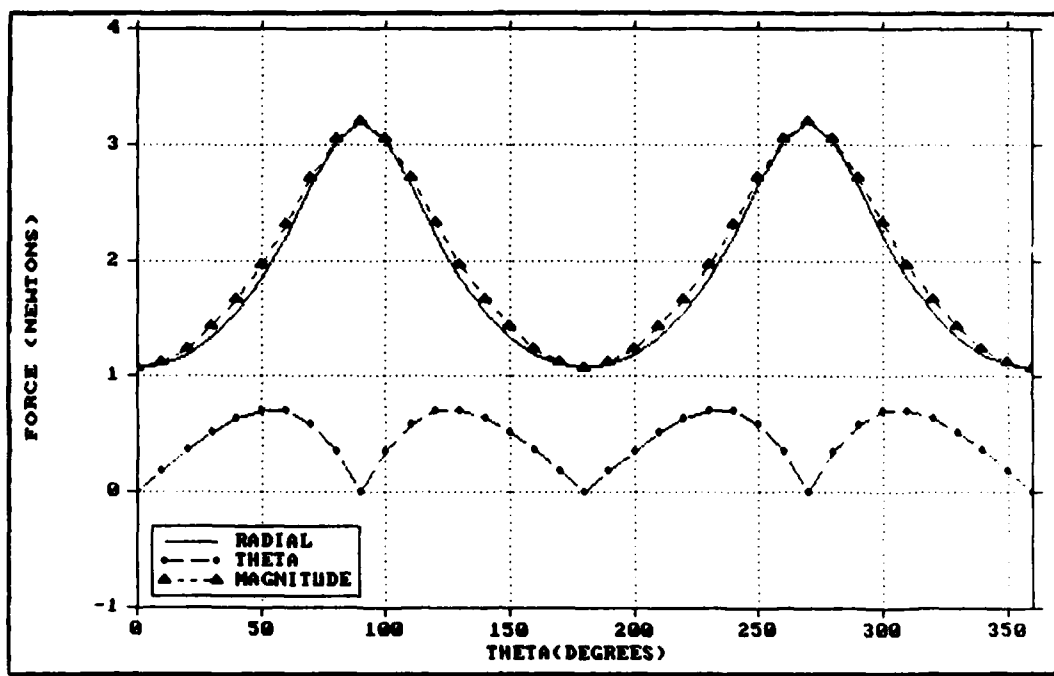


Figure 19. Magnetic Forces for Case III (600 Kilometer Orbit)

Case IV: An Inertially Oriented Current Loop

In this situation the plane of the loop is maintained parallel to some inertial orientation. As long as the orientation can be defined in terms of the radial and theta components of the geomagnetic field lines, a solution can be found. For the purposes of illustration for this thesis, the orientation will be maintained parallel to the equatorial geomagnetic plane. Gamma (Γ) is the angle between the plane of the loop and the radial direction and will be used to define the orientation as shown in Figure 12. When over the pole the orientation is the same as Case I. At the equator it resembles Case II or III but with the current flowing in the opposite direction.

The force is again given by Eq (43). Gamma is 90 degrees over the pole and zero at the equator. Therefore $\Gamma = 90-\theta$ so:

$$\cos(\Gamma) = \cos(90-\theta) = \sin(\theta) \quad (75)$$

$$\sin(\Gamma) = \sin(90-\theta) = \cos(\theta) \quad (76)$$

The expansion of the cross product matrix can therefore be expressed

$$\begin{aligned} d\mathbf{F} = idL\{ &B_r \sin(\Omega)\hat{\mathbf{R}} - B_\theta \sin(\Omega)\hat{\theta} \\ &+ [-B_r \cos(\Omega)\sin(\theta) + B_\theta \cos(\Omega)\cos(\theta)]\hat{\phi} \} \end{aligned} \quad (77)$$

The force in the radial direction is given by Eq (45)

$$F_R = \int dF_R \hat{\mathbf{R}} = \int ir \sin(\Omega) d\Omega B_r \quad (45)$$

Substituting Eq (37) for B_r and noting from Figure 16 that

$$\begin{aligned}\Delta R &= -r\sin(\Omega)\cos(\Gamma) \\ &= -r\sin(\Omega)\cos(90-\theta) \\ &= -r\sin(\Omega)\sin(\theta)\end{aligned}\quad (78)$$

and

$$\begin{aligned}\Delta \theta &= (-r/R)\sin(\Omega)\sin(\Gamma) \\ &= (-r/R)\sin(\Omega)\sin(90-\theta) \\ &= (-r/R)\sin(\Omega)\cos(\theta)\end{aligned}\quad (79)$$

the integral becomes:

$$\begin{aligned}F_R &= ir\sin(\Omega)d\Omega\{3(Re^3/R^4)g^0\sin(\theta)[-r\sin(\Omega)\sin(\theta)] \\ &\quad + (-Re/R)^3g^0\cos(\theta)[(-r/R)\sin(\Omega)\cos(\theta)]\}\end{aligned}\quad (80)$$

Resolving into two integrals, combining terms and pulling constants out of the integrand yields:

$$\begin{aligned}F_R &= -3\sin^2(\theta)(ir^2g^0Re^3/R^4)\int\sin^2(\Omega)d\Omega \\ &\quad + \cos^2(\theta)(ir^2g^0Re^3/R^4)\int\sin^2(\Omega)d\Omega\end{aligned}\quad (81)$$

Evaluating the integral around the current loop yields the force in the radial direction as

$F_{R1V} = (i\pi r^2 g^0 Re^3 / R^4)[\cos^2(\theta) - 3\sin^2(\theta)]$

(82)

The force in the theta direction is given by Eq (51):

$$F_\theta = \int dF_\theta \hat{\theta} = \int -irs\in(\Omega)d\Omega B_R \quad (51)$$

Substituting Eq (36) for B_R and recalling Eq (78) and (79) the integral expands to

$$\begin{aligned}F_\theta &= \int -irs\in(\Omega)d\Omega\{6(Re^3/R^4)g^0\cos(\theta)[-r\sin(\Omega)\sin(\theta)] \\ &\quad + 2(Re/R)^3g^0\sin(\theta)[(r/R)\sin(\Omega)\cos(\theta)]\}\end{aligned}\quad (83)$$

Resolving into two integrals, combining terms, and pulling constants out of the integrand yields:

$$F_T = 6\cos(\theta)\sin(\theta)ir^2g^0Re^3/R^4 \int \sin^2(\Omega)d\Omega + 2\sin(\theta)\cos(\theta)ir^2g^0Re^3/R^4 \int \sin^2(\Omega)d\Omega \quad (84)$$

Evaluating the integral around the loop gives the force in the theta direction

$$F_{TIV} = 8\cos(\theta)\sin(\theta)(i\pi r^2g^0Re^3/R^4) \quad (85)$$

The force in the phi (Φ) direction is zero due to a $\sin(\Omega)\cos(\Omega)$ term in the integrand. The radial, theta and total forces are shown in Figure 20 for Case IV. The magnitude is again representative of a 1000 meter radius current loop carrying 10 amps.

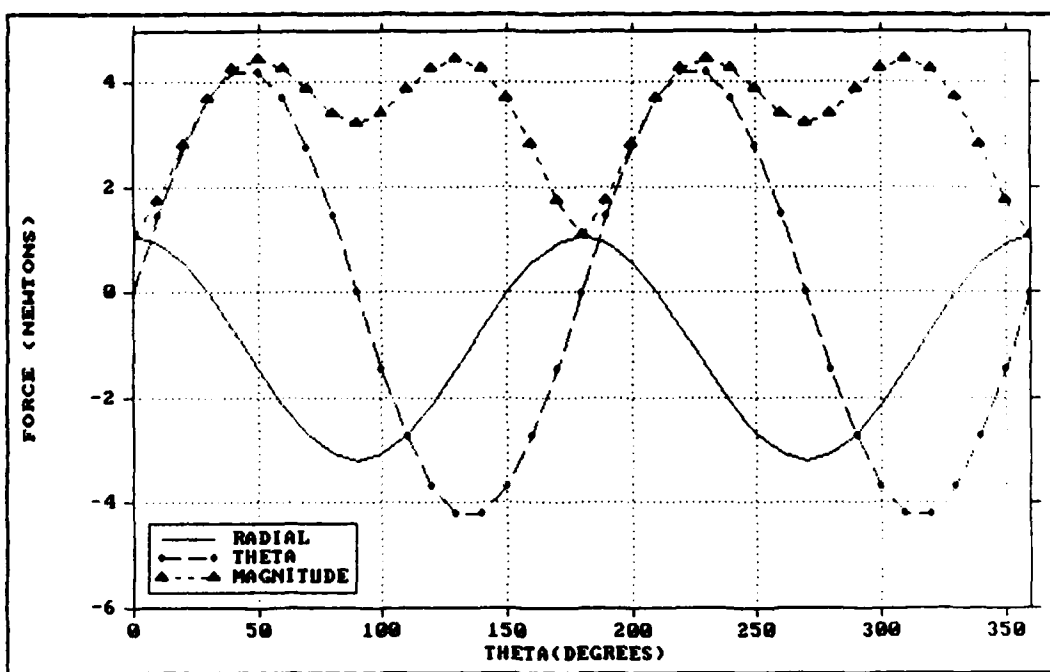


Figure 20. Magnetic Force for Case IV (600 Kilometer Orbit)

V. APPLICATION

The force alone tells little about the effect the current loop and geomagnetic field interaction have on a satellite. The force this technique can apply to a space system must be compared to other space propulsion systems.

Various characteristics are used to compare thruster performance. The generally recognized measures are: specific impulse (I_{sp}) - an overall performance comparison standard, characteristic exhaust velocity (c^*) - a measure of propellant combination and combustion chamber design, and thrust coefficient (C_F) - a measure of nozzle performance (Sutton, 1986:50,55). Since action-at-a-distance systems have no exhaust products and an infinite specific impulse, these traditional comparisons have little meaning. Some other comparison must be established. Other possibilities include total impulse ($\int F dt$), power-plant specific mass (kilograms per kilowatt), or acceleration capability (Sutton, 1986:21, Corliss, 1960:4).

From the standpoint of acceleration capability, the obvious comparison is with other low-thrust systems such as ion propulsion, however a comparison with chemical rockets can be made based on total (lifetime) impulse. Naturally, comparisons will have to be made for operation in similar environments - for instance "gravity-free", drag-free space.

Practically speaking it is the acceleration this force can produce to perturb the satellite that is of interest. The

acceleration stems from the relationship given by Newtons second law, that is, $F = ma$. Therefore, satellite system mass (m) must be known to assess the acceleration (a) available from a given force (F).

Some baseline satellite characteristics will be established. Assuming a satellite operating payload of approximately 3000 kilograms, the mass of the power supply, the current loop, the support structure, and the power conditioner must be added. The current loop mass is a function of the density of its material and size. Comparing nine gauge (2.91 millimeter diameter) wire for two common conductors, copper and aluminum, the following characteristics are given (CRC, 1973:F137-143): Copper has a current capacity of 30 amperes, a resistivity of 2.60 ohms per kilometer (at 20°C), and a mass of 58.98 kilograms per kilometer. Aluminum has a current capacity of 25 amperes, a resistivity of 4.26 ohms per kilometer, and a mass of 17.90 kilograms per kilometer. A 1000 meter radius loop of copper would have a mass of 371 kilograms and the same loop in aluminum would be 113 kilograms. From the standpoint of cost to launch, lighter materials are preferable to heavier. The high currents required in this system require thicker wire to reduce resistance. The more conductive wire will reduce ohmic heating, improving efficiency. A measure of merit used by Prall (1987:38) would be to look for the largest ratio of conductivity to density. It is apparent that little is lost

in terms of resistance and current capacity if aluminum wire is used rather than the heavier copper.

The power generation could be from a nuclear reactor or solar panels. Assuming solar cells were used, a reasonable attainable goal for solar panels is 250 watts per square meter and 20 kilograms per kilowatt (Sutton, 1986:498). To generate 25 kilowatts of power for the satellite systems and to drive a current of ten amps in the loop would require 100 square meters of solar cells and 500 kilograms of additional mass. Since optimal alignment with respect to the sun may not always be maintained and degradation of the solar cells will occur over time, doubling this to 200 square meters and 1000 kilograms provides a margin for continuing capability. A support structure for the current loop, a power conditioner, and accessories for the satellite could mass 5885 kilograms for a system mass of 10,000 kilograms. Using representative values of ten amperes for the current (i) and 1000 meters for the current loop radius (r) and the satellite mass arrived at above, the acceleration capability ranges from zero to $6 \times 10^{-4} g$'s and a watts per pound ratio of approximately one. Point A on Figure 21 compares this system to other typical values for different types of rocket engines.

Another comparison can also be made using total impulse. Total impulse (I_t) is the thrust force (F) integrated over the operating time (t); $I_t = \int F dt$, if the thrust is

constant and there are no stop and start transients, $I_t = Ft$.

From Figure 17-20 an average magnetic interactive force of two (2) newtons appears reasonable and assuming a twenty year lifetime, the total impulse is $1.26 \times 10^9 \text{ Kg-m/sec}$.

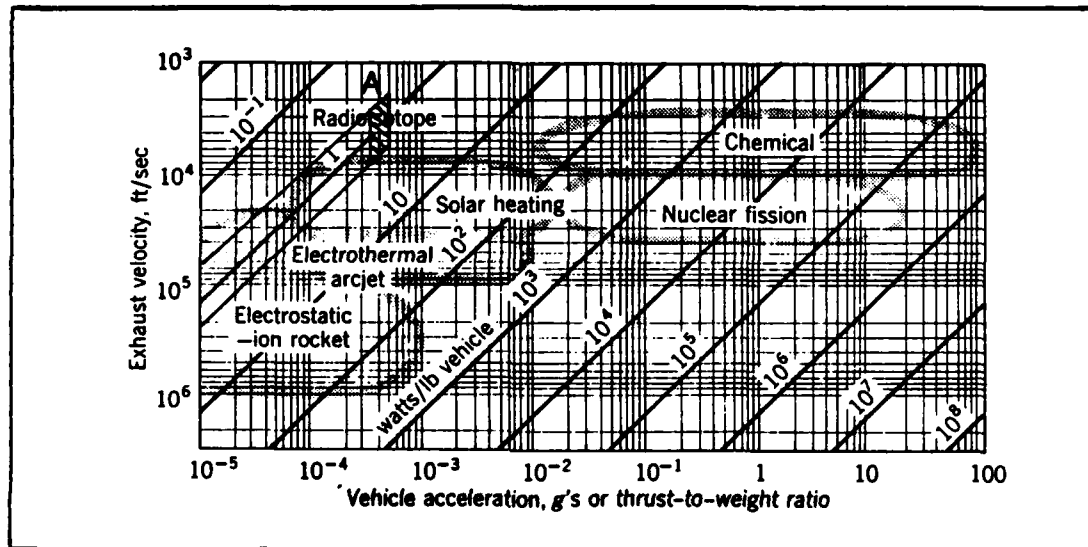


Figure 21. Operating Regimes of Various Thruster Systems
(Adapted from Sutton:32)

Using approximate values for thrust and burn time for various chemical rockets from Sutton (1986:31,196,210,216,263) and electric thrusters from Fearn (1982:160) total impulse can be calculated and is shown in Table I.

Table I. Comparison of Thrust, Burn Time, and Total Impulse for Various Rocket Engines

<u>Rocket Engine</u>	<u>Thrust (Nt)</u>	<u>Burn Time (s)</u>	<u>Total Impulse</u>
Saturn F-1	7.34E6	165	1.21E9
Saturn J-2	1.02E6	500	5.12E8
Shuttle Main	1.89E6	480	9.07E8
Minuteman	8.90E5	55	4.89E7
Lunar Module	4.63E4	800	3.70E7
General RCS	6.67E1	3600	2.40E5
Shuttle RCS	1.11E2	8.2E4	9.10E6
Kaufman 8 cm	4.90E-3	5.4E7	2.65E5
Kaufman 30 cm	2.10E-1	3.6E7	7.56E6

By this standard of comparison the magnetic field interaction appears very favorable, however, some of the comparisons are unrealistic in that the first five listed are primary propulsion designed to boost a vehicle out of a gravity well--something magnetic field interaction simply cannot accomplish. A more appropriate comparison would be to look at impulse deliverable over one orbit. Given an initially circular orbit of 600 kilometers, the orbital period is 5800 seconds. Table II shows impulse delivered in 5800 seconds for several thrusters.

Table II. Impulse Over One Orbit for Various Thrusters

<u>Thruster</u>	<u>Thrust (Nt)</u>	<u>Total Impulse</u>
Magnetic	2.0	1.16E4
Generic RCS	66.7	3.87E5
Shuttle RCS	111.2	6.44E5
Kaufman 8 cm	0.0049	2.84E1
Kaufman 30 cm	0.210	1.22E3

Perturbations

An external acceleration, that is, an acceleration other than the acceleration due to the central gravitational field that defines the orbit, will cause the parameters that define the orbit to vary with time. Ideally all disturbing forces must be determined and the net acceleration vectors calculated to specify how the orbit will change in the presence of those forces. Some of these disturbing forces that act on an orbiting satellite include aerodynamic drag, solar radiation pressure, earth's oblateness, induced electromagnetic force, solar wind, cosmic dust etc.

For this analysis, a comparison will be made between the magnetic force acting on the satellite and aerodynamic drag and solar radiation pressure. An estimate can be made of the change in orbital radius by equating the work done by the force over some portion of the orbit to the change in the specific mechanical energy of the orbit. In addition, Appendix A shows how the magnetic force can be applied using the Variation of Parameters technique to determine how the orbit can be altered by the magnetic force.

Magnetic Force vs Aerodynamic Drag

Aerodynamic drag forces are tangent to the orbit and opposite to the velocity. Since atmospheric particle density is a function of altitude, the aerodynamic drag forces are most noticeable at satellite perigee. Qualitatively, drag

effects are similar to an in-plane transfer maneuver applied at perigee: apogee height will be reduced as well as the semi-major axis and eccentricity. Perigee height, argument of perigee and inclination will remain approximately the same. The latter does not change since the aerodynamic drag effects are applied in-plane.

If atmospheric rotation is ignored--which is consistent with assuming a non rotating earth--the speed of the satellite relative to the atmosphere equals the inertial velocity. The aerodynamic drag force (F_d) can then be expressed as

$$F_d = \frac{1}{2} C_d \rho v^2 A \quad (86)$$

where

C_d = Drag coefficient
 ρ = Atmospheric density
 v = velocity of satellite
 A = frontal area of satellite

There are various frontal area configurations that could be considered to determine the drag coefficient. The solar panels could face into the direction of motion; the current loop support structure could be edge on or perpendicular to the orbit motion etc. The drag coefficient is approximately one (1) when the mean free path of the atmospheric molecules is small compared to the size of the satellite and two (2) when the mean free path is large compared to the size of the satellite (Roy, 1965:230). NASA SP 8058 gives a conservative drag coefficient of 2.6 for flat plate shapes. Assuming the drag coefficient to be a very conservative 3.0, the frontal

cross sectional area of the satellite system to be a minimum of 80 square meters and a maximum of 300 square meters, Table III shows the estimated aerodynamic force from 200 to 1000 kilometers.

Table III. Aerodynamic Drag Force at Various Altitudes

<u>Altitude(Km)</u>	<u>Density(Kg/m³)</u>	<u>Velocity(m/s)</u>	<u>Force(Nt)80/300m²</u>
200	2.541E-10	7.789E3	1.603/6.0123
400	2.803E-12	7.673E3	1.716E-2/6.436E-2
600	1.137E-13	7.562E3	6.762E-4/2.536E-3
800	1.136E-14	7.456E3	6.568E-5/2.463E-4
1000	3.561E-15	7.354E3	2.003E-5/7.511E-5

Figure 22 shows how the total magnetic force varies with altitude for Case III. Again magnitudes are representative of a 1000 meter radius current loop carrying 10 amps. As can be seen, the magnitudes of the magnetic force are all greater than the aerodynamic drag at altitudes over 400 kilometers.

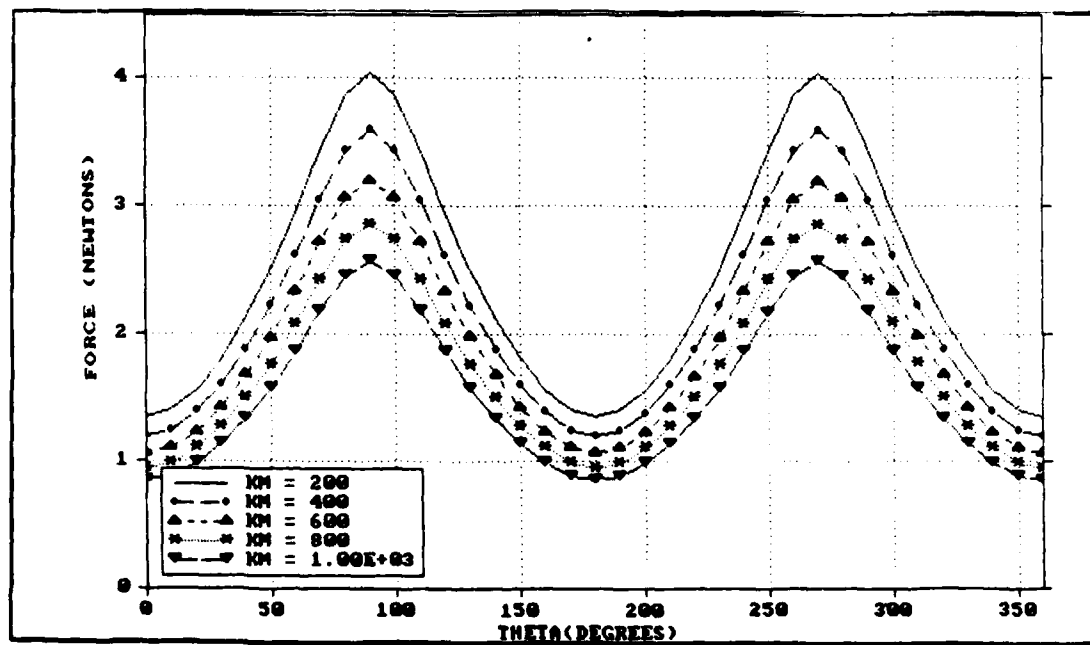


Figure 22. Magnitude of Total Magnetic Force for Case III

Solar Radiation Pressure

Sutton (1986:117) states that the solar radiation pressure on a given surface of a satellite near the earth's solar distance is

$$p = 4.5E-6 \cos(\theta)[(1-k_s)\cos(\theta) + 0.67k_d] \quad (87)$$

where

k_s = specular coefficient of reflectivity

k_d = diffuse coefficient of reflectivity

θ = angle between incident vector and surface normal vector

Typical values of 0.9 and 0.5 for k_s and k_d respectively for the body of the satellite and 0.25 and 0.01 for the solar panels are given in Sutton and NASA SP 8027. Using an approximate satellite body area of 25 square meters and effective solar array area of 80 to 300 square meters the solar radiation pressure is 3.214E-4 to 1.0704E-3 newtons. This force begins to dominates aerodynamic drag forces between 600 and 800 kilometers as shown in Figure 23.

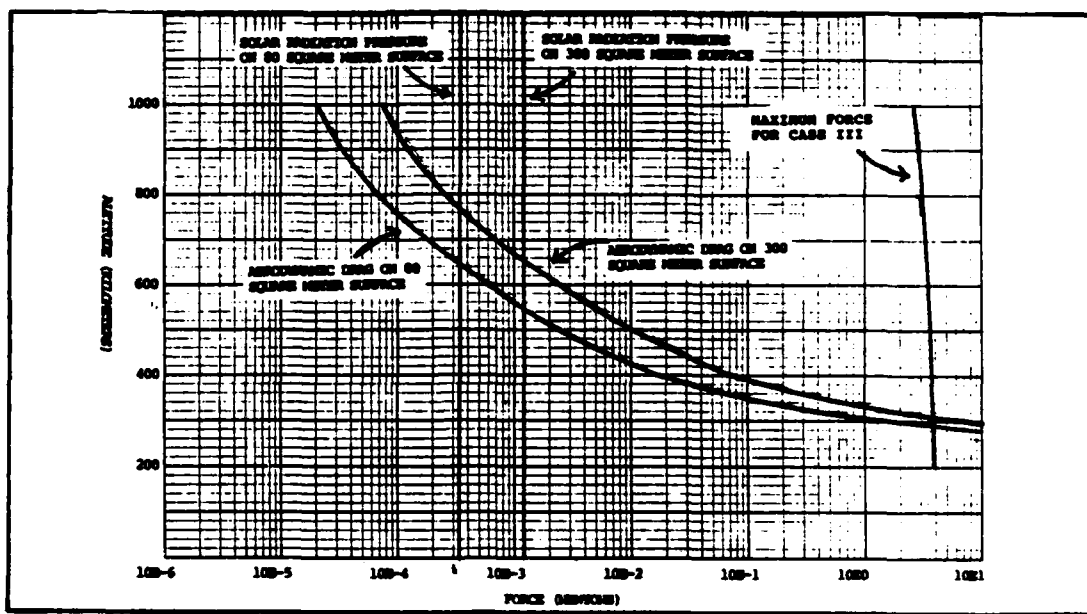


Figure 23. Aerodynamic Drag Vs Solar Radiation Pressure

Magnetic Thruster Operation

Applying low, continuously applied tangential thrust in the direction of satellite motion, potential energy rather than kinetic energy is added to the satellite. The satellite will progress to a higher, more energetic orbit, although one with less tangential velocity (Corliss, 1960:38). The work done by the force is the product of the force and the distance over which it is applied [$FRd\theta$]. This can be added to the specific mechanical energy of the orbit or equated to the change in energy of the orbit [$d/dR(-\mu/2R) = \mu/2R^2$]. Given that the satellite starts out in a circular orbit and a very low tangential force is applied, the satellite will follow a spiral trajectory to a higher orbit. The orbit will, however, continue to approximate a circle. Corliss gives the increase in orbit radius by the application of a small tangentially applied force as

$$dR = 2FR_e/g_0 m(R/R_e)^3 d\theta \quad (88)$$

where

R = orbital radius (m)
R_e = radius of the earth (m)
F = force (Nt)
m = mass of the satellite (kg)
g₀ = acceleration of gravity (m/s²)
θ = angle along the orbit (radians)

Introducing time from $V_s = Rd\theta/dt$, we have

$$dt = (R_e/g_0)^{1/2} (R/R_e)^{3/2} d\theta \quad (89)$$

Combining the two equations then gives

$$t = \frac{g_0 m R_e}{F(g_0)^{1/2}} [1/(R_0)^{1/2} - 1/(R)^{1/2}] \quad (90)$$

where

R = initial radius of satellite's orbit (m)
 R_0 = final radius of satellite's orbit (m)

Corliss shows that a satellite with a thrust to weight ratio of 10^{-4} (initially in a 500 kilometer circular orbit) can reach escape velocity in 92 days and 400 orbits. This is the same order of magnitude as the acceleration available due to the magnetic field interactive force. However, since the magnetic field strength drops off as the cube of the radius of the orbit, the applied force also decreases. While escape velocity cannot be achieved in ninety days, the orbit radius can be changed by approximately 1000 meters over one half of an orbit for a ten amp, 1000 meter radius current loop, starting in a 600 kilometer circular orbit. This orbital radius change assumes a constant force of two newtons applied in the tangential direction.

For the four orientations discussed in Chapter IV, the force varies in magnitude and is not totally applied in a tangential direction, therefore the orbit will not actually be a spiral but osculatory as it gains energy. If the orientation and current direction can be changed at will, higher average force levels are available. A more precise determination of the change in the orbital elements requires an extensive analysis using the variation of parameters. The appropriate equations are given in Appendix A.

VI. CONCLUSION

Summary

Several models exist to determine the geomagnetic field at any point around the earth. The simplest of these, and the one used herein to demonstrate the thesis concept, is the axial dipole. It was shown that the force acting on the current loop by the geomagnetic field can be calculated for any orientation of the current loop in orbit about the earth.

Given the assumptions in Chapter I and the constraints they represent, a number of conclusions can be drawn. The first, that a small net force exists on a current loop that extends over some gradient of the geomagnetic field, was anticipated, as well as the fact that it would scale proportionally to the area of the loop and the current the loop would carry. The fact that the net force would vary to the extent that it does with position and orientation was not expected.

As was shown in Table III and Figure 22, the magnetic force exceeds aerodynamic drag above approximately 300 kilometers. Even as solar radiation pressure begins to exceed aerodynamic drag above 700 kilometers, it, in turn, is still less than the magnetic force available for most of an orbit up to at least 1600 kilometers. The preeminent conclusion to this thesis, therefore, is that a current loop can be applied as a space thruster to change the specific

energy of a satellite and hence the satellite's orbital elements.

While several simplifying assumptions were made, they did not detract from the proof-of-concept. For instance, the simplification of the earth's magnetic field to a simple axial dipole was made for ease of analysis, but the method of analysis would be the same if an octopole or greater expansion of the infinite series was used. With only the first term of the geomagnetic field expansion being used there was no phi component of the magnetic field. Furthermore, only polar orbits were considered since there would be no force component in the phi direction, however, any orbit can be considered. The four orientations represented a building block approach to the analysis, but their selection covers all possible orientations and provide a stepping off point for the inclusion of the effects of torque on the loop. The non-rotating earth simplification was made for the sake of atmospheric drag calculations.

Some of the assumptions were made due to a lack of definitive engineering data and experience in the academic and engineering worlds. Specifically, the assumption of rigidity and power requirements and the dynamics of these structures. For proof of concept, however, these assumptions are tolerable, though subject to possible debate. The dynamics of large scale space structures and power generation in space will be answered in greater detail as the nation

ventures into the space station era of space exploitation and exploration.

Recommendations

Should this type of action-at-a-distance thruster actually be employed, a computer generated solution should carry the geomagnetic model to an octopole or even include all 80 terms of the IGRF model with coefficients updated by a follow-on to MAGSAT. This would be necessary for an accurate determination of the force the current loop would experience, as well as account for the changes that the geomagnetic field undergoes as opposed to a simple axial magnetic dipole.

Since one assumption made was the ability to maintain any desired orientation throughout the orbit, additional work should be done to determine the net force as the loop rotated due to the torque it would experience in the geomagnetic field. This would probably be oscillatory and approach a stabilization orientation similar to Case III. Another useful analysis would be to solve for the orientation that maintains the greatest force for any given position.

Since the effective use of this type of action-at-a-distance force depends on the advent of large scale space structures and large amounts of power, an initial application could perhaps be considered for an orbiting power generation satellite.

Appendix A: Variation of Parameters

Variation of Parameters is a computational method for calculating orbital elements. In the presence of a small perturbative force the orbital elements will change slowly with time. While other methods of calculating changes to an orbit maintain a constant reference orbit until rectification occurs, with variation of parameters the orbit changes are calculated continuously.

The following steps and equations (adapted from Bate and others, 1971:396-407,72) outline the procedures necessary to determine the actual change that will take place in a satellite's orbit when subject to a perturbative force.

1. Set initial conditions at time $t = t_0$ for position (\underline{r}) and velocity (\underline{v}) in the (I,J,K) reference frame (Figure 11).
2. Calculate the fundamental vectors ($\underline{h}, \underline{n}, \underline{e}$) at time $t = t_0$ where

$\underline{h} = \text{the angular momentum } (\underline{h} = \underline{r} \times \underline{v})$

$\underline{n} = \text{the node vector } (\underline{n} = \underline{K} \times \underline{h})$

$\underline{e} = \text{the eccentricity vector } (\underline{e} = 1/\mu[(v^2 - \mu/r)\underline{r} - (\underline{r} \cdot \underline{v})\underline{v}])$

3. Calculate the orbital elements at time $t = t_0$ where

$a = \text{the semi-major axis}$

$e = \text{the eccentricity}$

i = the inclination

Ω = longitude of ascending node

w = argument of periapsis

These are shown in Figure 11.

4. Compute the perturbative force at time $t = t_0$ and transform to the (R,S,W) system. These force components are given in Eq (50), (54), (62), (63), (70), (73), (82), and (85).
5. Compute the right hand side of da/dt , de/dt , di/dt , $d\Omega/dt$, dw/dt , dM_0/dt (as shown in steps 5-1 through 5-7 below).
6. Numerically integrate each equation from step five one time increment and step time counter.
7. Add the changes from step six to the old elements from step three.
8. Calculate the new position and velocity vectors (r and v) from the new elements.
9. Go to step four until reaching final time step.

Each of the preceding nine steps is expanded in the following series of steps and substeps:

1. Set initial conditions at $t = t_0$

$$\underline{r} = r_I \hat{I} + r_J \hat{J} + r_K \hat{K} \quad r = (r_I^2 + r_J^2 + r_K^2)^{1/2}$$
$$\underline{v} = v_I \hat{I} + v_J \hat{J} + v_K \hat{J} \quad v = (v_I^2 + v_J^2 + v_K^2)^{1/2}$$

2. Calculate the three fundamental vectors

$$2-1. \quad \mathbf{h} = \mathbf{r} \times \mathbf{v} = \begin{vmatrix} \hat{\mathbf{i}} & \hat{\mathbf{j}} & \hat{\mathbf{k}} \\ r_i & r_j & r_k \\ v_i & v_j & v_k \end{vmatrix}$$

$$= (r_j v_k - v_j r_k) \hat{\mathbf{i}} - (r_i v_k - v_i r_k) \hat{\mathbf{j}} + (r_i v_j - v_i r_j) \hat{\mathbf{k}}$$

$$= h_i \hat{\mathbf{i}} + h_j \hat{\mathbf{j}} + h_k \hat{\mathbf{k}} \quad h = (h_i^2 + h_j^2 + h_k^2)^{1/2}$$

$$2-2. \quad \mathbf{n} = \mathbf{k} \times \mathbf{h} = \begin{vmatrix} \hat{\mathbf{i}} & \hat{\mathbf{j}} & \hat{\mathbf{k}} \\ 0 & 0 & 1 \\ h_i & h_j & h_k \end{vmatrix}$$

$$= -h_j \hat{\mathbf{i}} + h_i \hat{\mathbf{j}}$$

$$= n_i \hat{\mathbf{i}} + n_j \hat{\mathbf{j}} + n_k \hat{\mathbf{k}} \quad n = (n_i^2 + n_j^2 + n_k^2)^{1/2}$$

$$2-3. \quad \underline{\mathbf{e}} = 1/\mu \{ [v^2 - (\mu/r)] \underline{\mathbf{r}} - (\underline{\mathbf{r}} \cdot \underline{\mathbf{v}}) \underline{\mathbf{v}} \}$$

$$= 1/\mu \{ [v^2 - (\mu/r)] (r_i \hat{\mathbf{i}} + r_j \hat{\mathbf{j}} + r_k \hat{\mathbf{k}})$$

$$- [(r_i v_i + r_j v_j + r_k v_k) (v_i + v_j + v_k)] \}$$

where $\mu = GM$

$$= e_i \hat{\mathbf{i}} + e_j \hat{\mathbf{j}} + e_k \hat{\mathbf{k}} \quad e = (e_i^2 + e_j^2 + e_k^2)^{1/2}$$

3. Calculate the orbital elements

$$3-1. \quad p(\text{semi-latus rectum}) = h^2/\mu$$

$$3-2. \quad e = |\underline{\mathbf{e}}|$$

$$3-3. \quad a = (1-e^2)/p$$

$$3-4. \quad i = \arccos h_k/h$$

$$3-5. \quad \Omega = \arccos n_i/n \quad (\text{if } n_j > 0, \text{ then } \Omega < 180^\circ)$$

$$3-6. \quad w = \arccos (\underline{\mathbf{n}} \cdot \underline{\mathbf{e}})/ne = (n_i e_i \hat{\mathbf{i}} + n_j e_j \hat{\mathbf{j}} + n_k e_k \hat{\mathbf{k}})/ne$$

$$= (-h_j e_i \hat{\mathbf{i}} + h_i e_j \hat{\mathbf{j}})/ne \quad (\text{if } e_k > 0, \text{ then } w < 180^\circ)$$

$$3-7. \quad \nu_0 \text{ (true anomaly at epoch)} = (\underline{\mathbf{e}} \cdot \underline{\mathbf{r}})/er$$

$$= (e_i r_i \hat{\mathbf{i}} + e_j r_j \hat{\mathbf{j}} + e_k r_k \hat{\mathbf{k}})/er$$

(if $\underline{\mathbf{r}} \cdot \underline{\mathbf{v}} > 0, \text{ then } \nu_0 < 180^\circ$)

$$\begin{aligned}
 3-8. \quad u_0 & (\text{argument of latitude at epoch}) = (\mathbf{n} \cdot \mathbf{r})/nr \\
 & = (n_i r_i \hat{\mathbf{i}} + n_j r_j \hat{\mathbf{j}} + n_k r_k \hat{\mathbf{k}})/nr \\
 & = (-h_j r_i + h_i r_j)/nr \quad (\text{if } r_k > 0, \text{ then } u_0 < 180^\circ)
 \end{aligned}$$

$$3-9. \quad l_0 \ (\text{true longitude at epoch}) = \Omega + w + v_0 = \Omega + u_0$$

4. Calculate the perturbative force

$$4-1. \quad K = (i\pi r^2 g^0 R e^3 / R^4)$$

$$4-2. \quad FR_1 = K \cos(\theta) \quad = F_R$$

$$4-3. \quad FT_1 = K 2\sin(\theta) \quad = F_S$$

$$4-4. \quad FR_2 = K 3\sin(\theta) \quad = F_R$$

$$4-5. \quad FT_2 = -K 6\cos(\theta) \quad = F_S$$

$$4-6. \quad FR_3 = K [3\sin(\theta)\sin(\beta) + \cos(\theta)\cos(\beta)] \quad = F_R$$

$$4-7. \quad FT_3 = K [2\sin(\theta)\cos(\beta) - 6\cos(\theta)\sin(\beta)] \quad = F_S$$

$$4-8. \quad FR_4 = K [\cos^2(\theta) - 3\sin^2(\theta)] \quad = F_R$$

$$4-9. \quad FT_4 = K [8\cos(\theta)\sin(\theta)] \quad = F_S$$

5. Compute the right hand side of the changes in the orbital elements.

$$5-1. \quad da/dt = [2e\sin(v)F_R/n(1-e^2)^{1/2}] + [2a(1-e^2)^{1/2}F_S/nr]$$

$$\begin{aligned}
 5-2. \quad de/dt &= [(1-e^2)^{1/2}\sin(v)F_R/na] \\
 &\quad + [(1-e^2)^{1/2}/na^2e]\{[a^2(1-e^2)/r] - r\}F_S
 \end{aligned}$$

$$5-3. \quad di/dt = rF_w \cos(u)/na^2(1-e^2)^{1/2} \quad (= 0 \text{ since } F_w = 0)$$

$$5-4. \quad d\Omega/dt = rF_w \sin(u)/na^2(1-e^2)^{1/2}\sin(i) \quad (= 0 \text{ since } F_w = 0)$$

$$5-5a. \quad (dw/dt)_R = -(1-e^2)^{1/2}\cos(v)F_R/nae$$

$$5-5b. \quad (dw/dt)_S = p/eh\{\sin(v)[1 + 1/[1+e\cos(v)]\}F_S$$

$$5-5c. \quad (dw/dt)_W = -rcot(i)\sin(u)F_w/na^2(1-e^2)^{1/2}$$

$$5-6. \quad dn/dt = (-3\mu/2na^4)da/dt$$

$$5-7. \frac{dM_0}{dt} = -1/na\{(2r/a) - [(1-e^2)/e]\cos(\nu)\}F_R$$

$$- [(1-e^2)/nae]\{1 + r/[a(1-e^2)]\}\sin(\nu)F_S$$

$$- t(dn/dt)$$

6. Numerically integrate each equation in step five above one time step.
7. Add the changes arrived at in step six to each of the old elements from step three.
8. Calculate new position and velocity vectors from the new elements arrived at in step seven. This is most easily done by calculating \underline{r} and \underline{v} in the perifocal coordinate and transforming back to the geocentric-equatorial (I,J,K) system.

$$8-1. \underline{r} = p/[1+ e\cos(\nu)]$$

$$8-2. \underline{r} = r\cos(\nu)\hat{\underline{P}} + r\sin(\nu)\hat{\underline{Q}}$$

$$8-3. \underline{v} = (\mu/r)^{1/2}\{-\sin(\nu)\hat{\underline{P}} + [e + \cos(\nu)]\hat{\underline{Q}}\}$$

8-4. Transform to (I,J,K)

$$\begin{vmatrix} ai \\ aj \\ ak \end{vmatrix} = R \begin{vmatrix} ap \\ aq \\ aw \end{vmatrix}$$

Let $c = \cos$
 $s = \sin$

$$R = \begin{vmatrix} c(\Omega)c(w)-s(\Omega)s(w)c(i) & -c(\Omega)s(w)-s(\Omega)c(w)c(i) & s(\Omega)s(i) \\ c(w)s(\Omega)+c(\Omega)s(w)c(i) & -s(\Omega)s(w)+c(\Omega)c(w)c(i) & -c(\Omega)s(i) \\ s(w)s(i) & c(w)s(i) & c(i) \end{vmatrix}$$

9. Go to step four until reaching final orbit or last time increment.

The steps are summarized in the following flow chart.

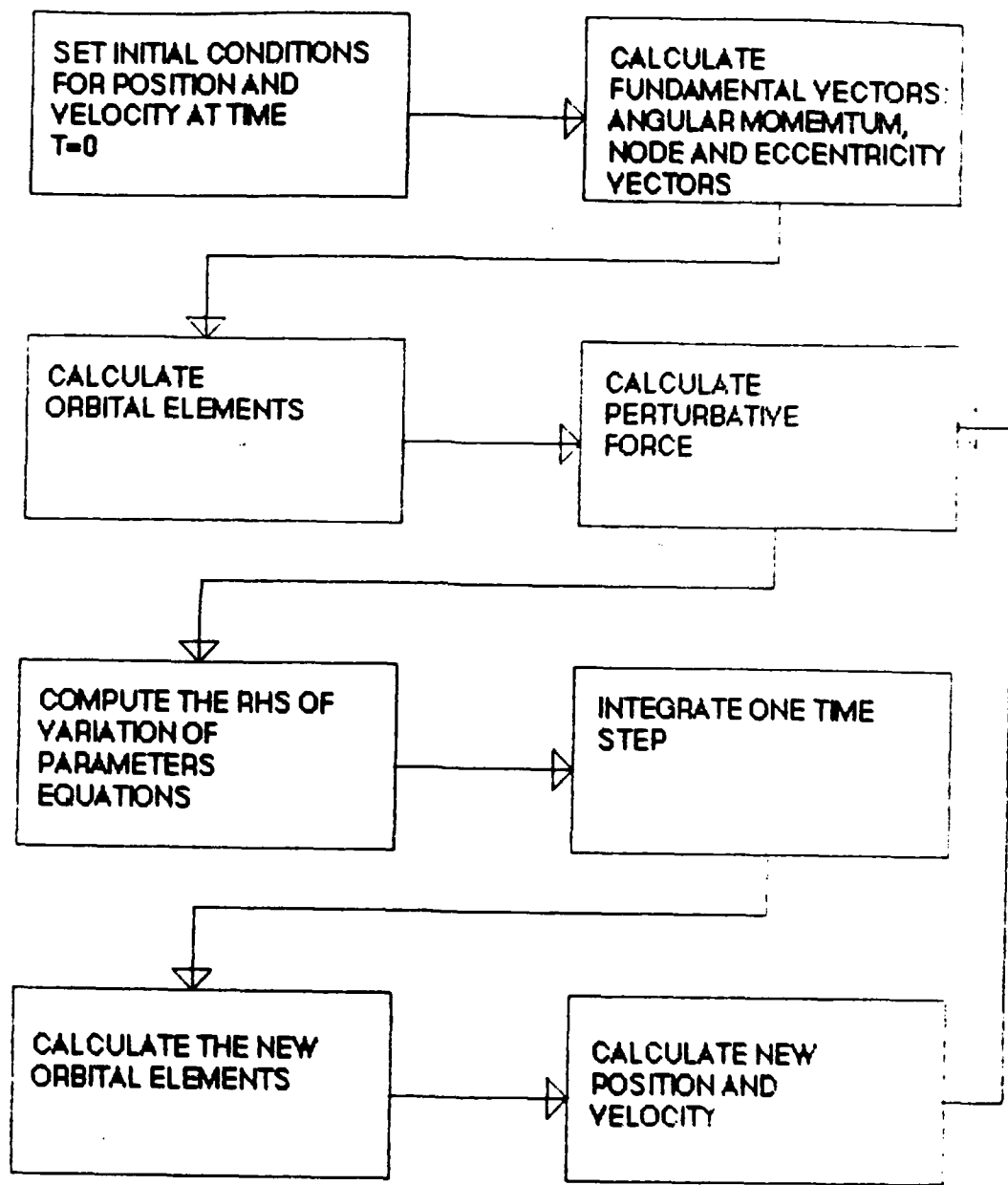


Figure 24. Variation of Parameters Flow Chart

Appendix B: Program for Calculating and Plotting Magnetic Force

The force calculations were made through the use of a software package called Powerpack. Created as a statistical applications software it is also capable of performing various formula calculations and has a simple but useful plotting routine. The following is the core of the magnetic force computation program.

```
*THIS PROGRAM CALCULATES THE GEOMAGNETIC FIELD AS A FUNCTION OF THE RADIAL;
*DISTANCE FROM THE CENTER OF THE EARTH AND COLATITUDE USING A SIMPLE;
*AXIAL DIPOLE MODEL FOR THE MAGNETIC FIELD. THIS PROGRAM THEN CALCULATES;
*THE FORCE ON A CURRENT LOOP IN THE GEOMAGNETIC FIELD. THE CURRENT I IS;
*ENTERED IN AMPS, THE CURRENT LOOP RADIUS r IS ENTERED IN METERS AND THE;
*ALTITUDE h IS ENTERED IN METERS. THERE ARE FOUR ORIENTATIONS TO BE;
*CONSIDERED AND TWO POSSIBLE CURRENT DIRECTIONS;
*-----;
*THIS FIRST SECTION DETERMINES WHAT VALUES ARE TO BE RETAINED UP TO A;
*MAX OF 10, AND THE INITIAL INPUT PARAMETERS;
*-----;
RETAIN THETA(DEGREES),BETAd,KM,F3;
prompt i,r,h,t;
define Re = 6370000;
define Rh = Re + h;
*-----;
*THIS SECTION CALCULATES THE GEOMAGNETIC FIELD AND ITS ORIENTATION;
*-----;
define Bt = -(6370000/Rh)^3*.31*sin(t);
define BR = -2*(6370000/Rh)^3*.31*cos(t);
define B = (Bt^2 + BR^2)^.5;
define s = (Bt);
define c = (BR);
define Beta = ArcTan(s,c);
*-----;
*THIS SECTION CALCULATES THE FORCE FOR THE DIFFERENT ORIENTATIONS;
*-----;
define K = (3.14159*r^2*i*.31*Re^3/Rh^4);
*-----;
*CASE 1: CURRENT LOOP PARALLEL TO EARTHS SURFACE;
*-----;
define FR1 = K*cos(t);
define Ft1 = K*2*sin(t);
define F1 = (FR1^2 + Ft1^2)^.5;
*-----;
*CASE 2: CURRENT LOOP PERPENDICULAR TO EARTHS SURFACE;
*-----;
define FR2 = K*3*sin(t);
define Ft2 = -K*6*cos(t);
define F2 = (FR2^2 + Ft2^2)^.5;
```

```

-----;
*CASE 3: CURRENT LOOP DIPOLE TANGENTIAL TO GEOMAGNETIC FIELD;
-----;
define FR3 = Abs(K*(3*sin(t)*sin(Beta)+cos(t)*cos(Beta));
define Ft3 = Abs(K*(2*cos(Beta)*sin(t)-6*cos(t)*sin(Beta));
define F3 = (FR3^2 + Ft3^2)^.5;
-----
*CASE 4: CURRENT LOOP MAINTAINING CONSTANT INERTIAL ATTITUDE;
-----;
define FR4 = K*(cos(t)*cos(t)-3*sin(t)*sin(t));
define Ft4 = 8*K*cos(t)*sin(t);
define F4 = (FR4^2 + Ft4^2)^.5;
-----
*REVERSING THE CURRENT DIRECTION;
-----;
define FR1B = FR1*(-1);
define Ft1B = Ft1*(-1);
define FR2B = FR2*(-1);
define Ft2B = Ft2*(-1);
define FR3B = FR3*(-1);
define Ft3B = (-1)*ABS(2*K*(3*cos(t)*sin(Beta)-sin(t)*cos(Beta)));
define FR4B = K*(3*sin(t)*sin(t)-cos(t)*cos(t));
define Ft4B = Ft4*(-1);
define THETA(DEGREES) = (180*t)/3.1415927;
define BETAd = 180 + (180*Beta)/3.1415927;
define KM = h/1000;
LET HSMIN = 0; LET HSMAX = 360;
LET VSMIN = 0; LET VSMAX = 4.5;
LET LEGXMIN = 0; LET LEGYMIN = 0.1;
SYMBOL @ 7 36 42 31;
YLABEL = FORCE (NEWTONS);
run;

```

BIBLIOGRAPHY

- Alfvén, Hannes, and Carl-Gunne Falthammar. Cosmical Electrodynamics. New York: Oxford University Press, 1963.
- Bate, Roger R. et al. Fundamentals of Astrodynamics. New York: Dover Publications, 1971.
- Chapman, Sydney and Julius Bartels. Geomagnetism. Oxford: Clarendon Press, 1940.
- Cheston, Warren B. Elementary Theory of Electric and Magnetic Fields. New York: John Wiley & Sons, 1964.
- Corliss, William R. Propulsion Systems for Space Flight. New York: McGraw-Hill Book Company, Inc., 1960.
- Dart, Francis E. Electricity and Electromagnetic Fields. Columbus: Merrill Books, Inc., 1966.
- Edelbaum, Theodore N. "Optimization Problems in Powered Space Flight," Proceedings of the AAAS/AAS Special Astronautics Symposium, Published in Vol. 9, Recent Developments in Space Flight Mechanics, AAS Science and Technology Series, Paul B. Richards, ed. Washington D.C.: AAS Publications, 1966, 113-132.
- Eller, Thomas J. "Magnetic Torques on Global Position System Satellites." The Journal of the Astronautical Sciences, 31, no. 2: 315-328 (1983).
- Evans, Howard E. and James Lange. Class notes for PHYS 519, The Space Environment. School of Engineering, Air Force Institute of Technology (AU), Wright-Patterson AFB OH, July 1987.
- Fairfield, Donald H., and Gilbert D. Mead. "Magnetospheric Mapping with a Quantitative Geomagnetic Field Model." Journal of Geophysical Research, 80, no. 4: 535-544 (February 1975).
- Fearn, D.G., "Electric Propulsion of Spacecraft." Journal of the British Interplanetary Society, vol. 35 (1982): 156-166.
- Herman, L.K. Closed Form Magnetic Quarter Orbit Switch Point Solution, 15 July 1977. Contract F04701-76-c-0077. El Segundo, CA: The Aerospace Corporation (AD-A048624).

- Halliday, David, and Robert Resnick. Fundamentals of Physics. New York: John Wiley & Sons, 1970.
- Handbook of Chemistry and Physics. (53rd Edition) Robert C. Weast, (ed.) Cleveland: The Chemical Rubber Company, 1973.
- Jackson, John D. Classical Electrodynamics. New York: John Wiley & Sons, 1967.
- Kaplan, Marshall H. Modern Spacecraft Dynamics & Control. New York: John Wiley & Sons, 1976.
- Klumper, D.M. Investigation of the Effects of External Current Systems on the MAGSAT Data Utilizing Grid Cell Modeling Techniques. 1 April 1982 - 1 July 1982. NASA Contract no. NAS5-26309. Richardson TX: Center for Space Sciences - University of Texas at Dallas, July 1982.
- Mead, Gilbert D., and Donald H. Fairfield. "A Quantitative Magnetospheric Model Derived from Spacecraft Magnetometer Data." Journal of Geophysical Research. 80, no. 4: 523-534 (February 1975).
- Roy, Archie E. The Foundations of Astrodynamics. New York: The Macmillian Company, 1965.
- Spacecraft Aerodynamic Torques. NASA SP8058, January 1971. (N 71-25935).
- Spacecraft Magnetic Torques. NASA SP8018, March 1969. (N 69-30339).
- Spacecraft Radiation Torques. NASA SP8027, October 1969. (N 71-24312).
- Stacy, Frank D. Physics of the Earth. New York: John Wiley & Sons, 1969.
- Stern, D. P. Representation of Magnetic Fields in Space. Goddard Spaceflight Center Report x-602-75-57, March 1975.
- Stuhlinger, Ernst. Ion Propulsion for Space Flight. New York: McGraw Hill Book Company, 1964.
- Sutton, George P. Rocket Propulsion Elements. New York: John Wiley & Sons, 1986.
- Thomson, William T. Introduction to Space Dynamics. New York: Dover Publications, 1986.

Wertz, James R. ed. Spacecraft Attitude Determination and Control. Dordrecht, Holland: D. Reidel Publishing Company, 1985.

White, Stephen R. Space Physics. New York: Gordon & Breach Science Publishers, 1970.

Vita

Major Stephen R. Hildenbrandt [REDACTED]

[REDACTED] in 1973 [REDACTED] attended Oregon State University, from which he received the degree of Bachelor of Science in General Science in June 1977. Upon graduation, he received a commission in the USAF through the AFROTC program. He was employed as a physical science assistant for the U.S. Army Corps of Engineers, Coastal Engineering Research Center, Ft. Belvoir, Virginia, until called to active duty in October 1977. He completed navigator training and received his wings in June 1978. He then served as an F-111D Weapon Systems Officer in the 524th and 522nd Tactical Fighter Squadrons, Cannon AFB, New Mexico, an F-111E Instructor Weapon Systems Officer in the 55th Tactical Fighter Squadron, RAF Upper Heyford, England, an F-4 and F-111 Flight Test Weapon Systems Officer in the 3246 Test Wing, Eglin AFB, Florida, and a Flight Safety Officer in the Armament Division, Eglin AFB, Florida, until entering the School of Engineering, Air Force Institute of Technology, in June 1987.

[REDACTED]

[REDACTED]

[REDACTED]

[REDACTED]

UNCLASSIFIED
SECURITY CLASSIFICATION OF THIS PAGE

Form Approved
OMB No. 0704-0188

REPORT DOCUMENTATION PAGE

1a. REPORT SECURITY CLASSIFICATION UNCLASSIFIED		1b. RESTRICTIVE MARKINGS	
2a. SECURITY CLASSIFICATION AUTHORITY		3. DISTRIBUTION/AVAILABILITY OF REPORT Approved for public release; distribution unlimited	
2b. DECLASSIFICATION/DOWNGRADING SCHEDULE			
4. PERFORMING ORGANIZATION REPORT NUMBER(S) AFIT/GSO/ENP/88D-3		5. MONITORING ORGANIZATION REPORT NUMBER(S)	
6a. NAME OF PERFORMING ORGANIZATION School of Engineering	6b. OFFICE SYMBOL (If applicable) AFIT/ENS	7a. NAME OF MONITORING ORGANIZATION	
6c. ADDRESS (City, State, and ZIP Code) Air Force Institute of Technology Wright-Patterson AFB, OH 45433-6583		7b. ADDRESS (City, State, and ZIP Code)	
8a. NAME OF FUNDING/SPONSORING ORGANIZATION	8b. OFFICE SYMBOL (If applicable)	9. PROCUREMENT INSTRUMENT IDENTIFICATION NUMBER	
8c. ADDRESS (City, State, and ZIP Code)		10. SOURCE OF FUNDING NUMBERS	
		PROGRAM ELEMENT NO.	PROJECT NO.
		TASK NO.	WORK UNIT ACCESSION NO.
11. TITLE (Include Security Classification) GEO MAGNETIC FIELD ENERGY AS A SOURCE OF THRUST			
12. PERSONAL AUTHOR(S) Stephen R. Hildenbrandt, B.S., Major, USAF			
13a. TYPE OF REPORT MS Thesis	13b. TIME COVERED FROM _____ TO _____	14. DATE OF REPORT (Year, Month, Day) 1988 December	15. PAGE COUNT 95
16. SUPPLEMENTARY NOTATION			
17. COSATI CODES	18. SUBJECT TERMS (Continue on reverse if necessary and identify by block number) → Magnetic Forces; Space Propulsion; Geomagnetic Field		
FIELD	GROUP	SUB-GROUP	
20	03		
22	02		
19. ABSTRACT (Continue on reverse if necessary and identify by block number)			
Thesis Advisor: Lt Col Howard E. Evans Instructor of Physics Department of Engineering Physics			
20. DISTRIBUTION/AVAILABILITY OF ABSTRACT <input checked="" type="checkbox"/> UNCLASSIFIED/UNLIMITED <input type="checkbox"/> SAME AS RPT <input type="checkbox"/> DTIC USERS		21. ABSTRACT SECURITY CLASSIFICATION UNCLASSIFIED	
22a. NAME OF RESPONSIBLE INDIVIDUAL Howard E. Evans, Instructor of Physics		22b. TELEPHONE (Include Area Code) (513) 255-2012	22c. OFFICE SYMBOL AFIT/ENP

Approved for release in
Accordance with AFR 199-1
BSP/SPM/EMC
12 Jan 1987